



# City Research Online

## City St George's, University of London

**Citation:** Liu, X., Kassem, H. I. & Banerjee, J. R. (2016). An exact spectral dynamic stiffness theory for composite plate-like structures with arbitrary non-uniform elastic supports, mass attachments and coupling constraints. *Composite Structures*, 142, pp. 140-154. doi: 10.1016/j.compstruct.2016.01.074

This is the accepted version of the paper.

This version of the publication may differ from the final published version. To cite this item please consult the publisher's version.

**Permanent repository link:** <https://openaccess.city.ac.uk/id/eprint/15562/>

**Link to published version:** <https://doi.org/10.1016/j.compstruct.2016.01.074>

**Copyright and Reuse:** Copyright and Moral Rights remain with the author(s) and/or copyright holders. Copies of full items can be used for personal research or study, educational, or not-for-profit purposes without prior permission or charge, unless otherwise indicated, provided that the authors, title and full bibliographic details are credited, a hyperlink and/or URL is given for the original metadata page and the content is not changed in any way. For full details of reuse please refer to [City Research Online policy](#).

Manuscript Number: COST-D-15-02131R1

Title: An exact spectral dynamic stiffness theory for composite plate-like structures with arbitrary non-uniform elastic supports, mass attachments and coupling constraints

Article Type: Full Length Article

Keywords: spectral dynamic stiffness method (SDSM); composite plate-like structures; non-uniform elastic supports and mass attachments; non-uniform elastic coupling constraints; exact modal analysis; arbitrary boundary conditions

Corresponding Author: Dr. Xiang Liu, Ph.D.

Corresponding Author's Institution: City University London

First Author: Xiang Liu, Ph.D.

Order of Authors: Xiang Liu, Ph.D.; Hassan I Kassem; Jnan R Banerjee, Ph.D.

Abstract: This paper presents an exact spectral dynamic stiffness (SDS) theory for composite plates and plate assemblies with arbitrary non-uniform elastic supports, mass attachments and elastic coupling constraints. The theory treats the above supports, attachments and constraints in a sufficiently general, but accurate manner, which can be applied to various SDS formulations as well as classical dynamic stiffness formulations for both modal and dynamic response analysis. The methodology is concise but can be easily applied to complex plate-like structures with any arbitrary boundary conditions. It retains all the advantages of a recently developed SDS method which gives exact results with excellent computation efficiency. The results computed by the present theory are validated against published results. In order to demonstrate the practical applicability of the theory, three wide ranging engineering composite structures are investigated. For benchmarking purposes, results computed from the current theory are accurate up to the last figure quoted.

Response to Reviewers: Detailed Response to Reviewers

Spectral-dynamic stiffness theory for modal analysis of composite plate-like structures with arbitrary non-uniform elastic supports, coupling constraints and mass attachments Composite Structures

Revised title "An exact spectral dynamic stiffness theory for composite plate-like structures with arbitrary non-uniform elastic supports, mass attachments and coupling constraints"

X. Liu, H.I. Kassem and J.R. Banerjee

Ref: COST-D-15-02131

The authors are grateful to the reviewer for his/her careful and studied assessment of the paper. By taking all of the reviewer's comments into account the paper has now been thoroughly revised and the revisions are shown in red in the Marked version. A point-by-point reply to the reviewer's comments is given below.

Reply to the reviewer:

Reviewer: The paper is interesting and well written. Tables need to be enlarged but it could be part of the editorial process.

Reply: The authors are grateful to the reviewer's comment supporting the publication of the paper. Tables are small in the manuscript but should fit well with the final layout in Composite Structures, we would like to leave it to the editorial process as indicated by the reviewer.

Reviewer: The following point could make the paper more attractive: Second author has made excellent contribution in the past on DSM nevertheless he has introduced more recent contribution in which DSM has been used in conjunction with refined theories based on Unified Formulation, some of these were co-authorized by Boscolo, by Fazzolari and by Pagani. A discussion of these contribution would make this paper more complete as well as the use of these latter contribution to make major assessment of the procedure proposed in this article.

Reply: The authors are appreciative of the reviewer's instructive comments and for reminding them of several previous contributions on the DSM made by the senior author. Discussion on these contributions in conjunction with refined theories such as the Carrera's Unified Formulation (CUF) is now provided in the Introduction section and also in a new section, i.e., Section 2.2.3. Thanks to the reviewer's instructive comments, the authors realise that the theory proposed in this paper could be applied not only to the SDSM but also to the classical DSM, e.g., the DSM in conjunction with CUF as mentioned by the reviewer. The description of how to apply the current theory to the classical DSM is now added in the additional Section 2.2.3, which has broadened the appeal of the paper and no-doubt extended the applicability of the theory in a much wider context.

The authors are grateful to the reviewer for his/her insightful reading and suggestions which have improved the paper.

Dear Professor Ferreira,

**Ref: COST-D-15-02131 An exact spectral dynamic stiffness theory for composite plate-like structures with arbitrary non-uniform elastic supports, mass attachments and coupling constraints**

Professor Banerjee, Mr Kassem and I would be grateful if the above paper is considered for publication in Composite Structures. This is the **revised manuscript**. By taking all of the reviewer's comments into account, the paper has now been thoroughly revised and resubmitted. An additional marked version is also submitted with all revised parts shown in red.

We look forward to hearing from you in due course.

Yours sincerely,

Dr X. Liu

[Xiangliu06@gmail.com](mailto:Xiangliu06@gmail.com), [Xiang.liu.5@city.ac.uk](mailto:Xiang.liu.5@city.ac.uk)

## Detailed Response to Reviewers

---

### **Spectral-dynamic stiffness theory for modal analysis of composite plate-like structures with arbitrary non-uniform elastic supports, coupling constraints and mass attachments Composite Structures**

**Revised title “An exact spectral dynamic stiffness theory for composite plate-like structures with arbitrary non-uniform elastic supports, mass attachments and coupling constraints”**

X. Liu, H.I. Kassem and J.R. Banerjee

**Ref: COST-D-15-02131**

The authors are grateful to the reviewer for his/her careful and studied assessment of the paper. By taking all of the reviewer’s comments into account the paper has now been thoroughly revised and the revisions are shown in red in the **Marked version**. A point-by-point reply to the reviewer’s comments is given below. (Reviewer’s comments are shown in italics.)

***Reply to the reviewer:***

*The paper is interesting and well written. Tables need to be enlarged but it could be part of the editorial process.*

Reply: The authors are grateful to the reviewer’s comment supporting the publication of the paper. Tables are small in the manuscript but should fit well with the final layout in Composite Structures, we would like to leave it to the editorial process as indicated by the reviewer.

*The following point could make the paper more attractive:*

*Second author has made excellent contribution in the past on DSM nevertheless he has introduced more recent contribution in which DSM has been used in conjunction with refined theories based on Unified Formulation, some of these were co-authored by Boscolo, by Fazzolari and by Pagani. A discussion of these contribution would make this paper more complete as well as the use of these latter contribution to make major assessment of the procedure proposed in this article.*

Reply: The authors are appreciative of the reviewer’s instructive comments and for reminding them of several previous contributions on the DSM made by the senior author. Discussion on these contributions in conjunction with refined theories such as the Carrera’s Unified Formulation (CUF) is now provided in the Introduction section and also in a new section, i.e., Section 2.2.3. Thanks to the reviewer’s instructive comments, the authors realise that the theory proposed in this paper could be applied not only to the SDSM but also to the classical DSM, e.g., the DSM in conjunction with CUF as mentioned by the reviewer. The description of how to apply the current theory to the classical DSM is now added in the additional Section 2.2.3, which has broadened the appeal of the paper and no-doubt extended the applicability of the theory in a much wider context.

The authors are grateful to the reviewer for his/her insightful reading and suggestions which have improved the paper.

1  
2  
3  
4  
5  
6  
7  
8  
9  
10  
11  
12  
13  
14  
15  
16  
17  
18  
19  
20  
21

# An exact spectral dynamic stiffness theory for composite plate-like structures with arbitrary non-uniform elastic supports, mass attachments and coupling constraints

22  
23  
24  
25  
26  
27  
28  
29  
30  
31  
32  
33  
34  
35  
36  
37  
38  
39  
40  
41  
42  
43  
44  
45  
46

X. Liu\*, H.I. Kassem, J.R. Banerjee

*School of Mathematics, Computer Science & Engineering, City University London,  
London EC1V 0HB, UK*

---

## Abstract

24  
25  
26  
27  
28  
29  
30  
31  
32  
33  
34  
35  
36  
37  
38  
39  
40

This paper presents an exact spectral dynamic stiffness (SDS) theory for composite plates and plate assemblies with arbitrary non-uniform elastic supports, mass attachments and elastic coupling constraints. **The theory treats the above supports, attachments and constraints in a sufficiently general, but accurate manner, which can be applied to various SDS formulations as well as classical dynamic stiffness formulations for both modal and dynamic response analysis.** The methodology is concise but can be easily applied to complex plate-like structures with any arbitrary boundary conditions. It retains all the advantages of a recently developed SDS method which gives exact results with excellent computation efficiency. The results computed by the present theory are validated against published results. In order to demonstrate the practical applicability of the theory, three wide ranging engineering composite structures are investigated. For benchmarking purposes, results computed from the current theory are accurate up to the last figure quoted.

41  
42  
43  
44  
45

*Keywords:* spectral dynamic stiffness method (SDSM); composite plate-like structures; non-uniform elastic supports and mass attachments; non-uniform elastic coupling constraints; exact modal analysis; arbitrary boundary conditions

---

## 1. Introduction

47  
48  
49  
50  
51  
52  
53  
54

Dynamic analysis of plate-like structures with arbitrary non-uniform elastic supports (Fig.1(a)), mass attachments (Fig. 1(b)) and elastic coupling constraints (Fig.1(c)) has always been a challenging problem in many engineering areas. Such

---

55  
56  
57  
58  
59  
60  
61  
62  
63  
64  
65

\*Corresponding author

*Email address:* xiangliu06@gmail.com (X. Liu)

an analysis is important to avoid resonance or undesirable dynamic response, control acoustic emission and power flow [1], analyse the effects of cracks [2] or damaged boundaries [3] for identifying the location and destructiveness of these cracks and damages, and many others. The applicability of the proposed theory include, but not limited to, buildings, bridges, ships, aeroplanes, space structures, armoured vehicles, automobiles, machines, robots, optical beam pointing systems and so on. Non-uniform elastic supports, mass attachments and elastic coupling constraints are expected to change the dynamic behaviour of a structure significantly. It is timely and pertinent to review briefly the published work focused on the above three general types of non-classical boundary conditions (BC) and/or continuity conditions (CC). Fig. 1 depicts the above three general types of BC and/or CC corresponding to the Kirchhoff plate theory which serve as illustrating examples.

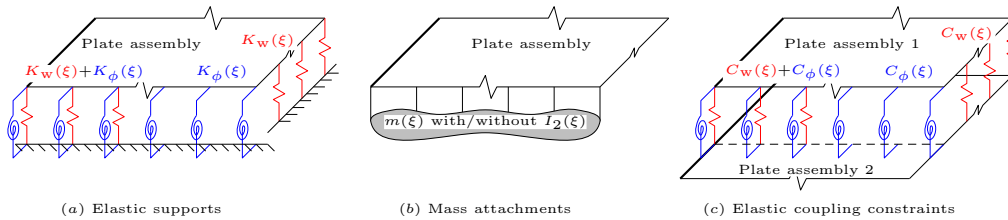


Figure 1: Three general types of non-classical boundary and/or continuity conditions (the cases corresponding to the Kirchhoff plate theory are used here for illustrating purposes) covered by the theory of this paper: (a) Elastic supports with non-uniform translational ( $K_w(\xi)$ ) and/or rotational ( $K_\phi(\xi)$ ) stiffnesses, (b) Mass attachments with non-uniform mass distribution  $m(\xi)$  and with/without non-uniform rotatory inertia  $I_2(\xi)$  and (c) Elastic coupling constraints with non-uniform translational  $C_w(\xi)$  and/or rotational  $C_\phi(\xi)$  coupling stiffnesses.

A wide range of methods have been proposed in the literature for free vibration of plates with elastic supports (see Fig.1(a)) but they are generally limited to *uniform* distribution [4–12]. One of the most widely used methods in this endeavour is the Ritz method [4–8], which is generally limited to uniformly distributed elastic supports due to the admissible functions adopted in the variable separable assumptions. Other methods such as the Fourier series based analytical method [9, 10], the finite strip method [11, 12] also appear to have similar limitations. The treatment of non-uniform elastic supports is obviously much more demanding when using any established method. Understandably, only a few research has attempted such problems [3, 13–18]. However, most of the published methods have limitations of different natures. Some methods can only be applied to plates with restricted boundary conditions. For example, the Spectral Collocation [3] and the Discrete Singular Convolution [17] methods appear to be limited to non-uniform rotational elastic supports and they have problems with non-uniform translational elastic supports and/or when any free edge is encountered. Moreover,

1  
2  
3  
4  
5 the results computed by most of these methods do not seem to be sufficiently ac-  
6 curate. This is mainly due to the numerical instability which generally occurs and  
7 prevents these methods from computing more accurate results by using higher or-  
8 der basis functions. Additionally, most of the existing methods are only applied  
9 to single plates [3, 13–19] and very few are applied to plates with intermediate  
10 uniform elastic supports [6, 7]. The application to more complex plate assemblies  
11 with non-uniform elastic supports is no doubt a difficult task when using most of  
12 the existing analytical methods.  
13  
14

15 Even though a lot of research on plates with point mass attachments has been  
16 reported [7, 20–23], there are very few publications on line mass attachments (see  
17 Fig. 1(b)) and that too are limited to *uniformly* distributed ones [24, 25]. (Note  
18 that point mass attachments can be considered as a special case of non-uniform  
19 line mass attachment.) The problem of non-uniformly distributed mass attach-  
20 ments (non-uniform  $m(\xi)$  and/or  $I_2(\xi)$  in Fig. 1(b)) has not been attempted in  
21 any great detail, although it has admittedly many applications in engineering. For  
22 example, an engine or a missile attached to an aircraft wing can be idealised as  
23 non-uniformly distributed mass with non-uniform rotatory inertia. Also, the shear  
24 wall structures of multi-story buildings can be modelled as plates placed verti-  
25 cally and subjected to non-uniform line mass and spring attachments representing  
26 the dynamic effects of the floors. The only reported research activities on plates  
27 subjected to line mass attachments are all restricted to cases with very simple  
28 boundary conditions, and furthermore the line mass attachments are considered to  
29 be uniformly distributed [24, 25] as opposed to non-uniform distribution. To the  
30 best of the authors' knowledge, there is no published literature for plate vibration  
31 with non-uniformly distributed mass attachments.  
32  
33

34 Solving the vibration problem of plate assemblies with elastic coupling con-  
35 straints (see Fig. 1(c)) is even more challenging, which has received rather sporadic  
36 attention [26]. Du et al [26] used a certain modified double Fourier series in the  
37 Rayleigh-Ritz method which was applied to two coupled plates with *uniform* elas-  
38 tic coupling constraints (constant  $C_w$  and  $C_\phi$ ). However, the formulation of this  
39 type is quite tedious even when applied to a model comprising only two coupled  
40 isotropic plates with uniform elastic constraints. Moreover, the results computed  
41 by such a method [26] are not really accurate. One of the reasons for this might  
42 be the numerical instability, which seems to be a stumbling block for this method  
43 when applied to more general cases of complex structures. Any non-uniform elas-  
44 tic coupling constraints ( $C_w(\xi)$  and  $C_\phi(\xi)$  as in Fig. 1(c)) could lead to even more  
45 serious numerical instability problems when using this method.  
46  
47

48 Against the above background, an exact spectral dynamic stiffness (SDS) the-  
49 ory is developed covering all of the above three general types of non-uniform  
50 boundary conditions (BC) and/or continuity conditions (CC) as illustrated in Fig.  
51 1. The development of the current theory is based on a recently developed spec-  
52  
53  
54  
55  
56  
57

1  
2  
3  
4  
5 tral dynamic stiffness method (SDSM) [27–29] with significant extensions to deal  
6 with the aforementioned three general types of non-uniform BC and/or CC along  
7 any of the line nodes of a composite plate assembly. These proposed enhance-  
8 ments have many engineering applications as mentioned earlier. Additionally, the  
9 theory inherits all the merits of the recently developed SDSM [27–29] including  
10 the high accuracy, computational efficiency and robustness. For instance, the cur-  
11 rent method has as much as 100-fold advantage of computational speed over the  
12 conventional finite element method. Any required natural frequency within the  
13 range of from low to high frequencies can be computed by the proposed theory  
14 with any desired accuracy. The theory is versatile and the composite plate as-  
15 semblies can of course, be subjected to any arbitrary boundary conditions in the  
16 present method.  
17  
18

19  
20 The SDS matrices for any arbitrarily distributed elastic supports and/or mass  
21 attachments and/or elastic coupling constraints are formulated in a concise man-  
22 ner and the theory is capable of handling simple as well as complex structures.  
23 Essentially, the development of such SDS matrices originates from expressing  
24 both sides of the corresponding constraint equations in terms of modified Fourier  
25 series [30]. The developed SDS matrices of the above non-uniform BC and/or CC  
26 are superposed directly onto the corresponding components of the SDS matrix of  
27 the composite plate-like structure. The formulation procedure can be regarded as  
28 a series-based exact formulation in a sense similar to that of the SDSM [27, 28].  
29 **It should be noted that the current SDS theory is complete general so that it can**  
30 **be applied to different SDS formulations based on different governing differential**  
31 **equations (GDE), e.g. [27–29, 31]. Of course, the theory can be degenerated, as a**  
32 **special case, to be applied to classical dynamic stiffness method (DSM) based on**  
33 **different GDE, e.g., those in conjunction with refined theories like Carrera’s Uni-**  
34 **fied formulation [32–36], for more details see Section 2.2.3. Moreover, the current**  
35 **theory can be used not only in modal analysis but also in dynamic response anal-**  
36 **ysis, but the focus of this paper is on modal analysis. As the solution technique,**  
37 **an enhanced Wittrick-Williams algorithm [27, 28] is applied to the superposed**  
38 **SDS matrix to compute any required natural frequencies to any desired accuracy.**  
39 **For illustrative purposes, the current theory is applied to a number of engineering**  
40 **problems. It should be noted that all SDSM results presented in this paper (shown**  
41 **in bold) are accurate up to the last figures quoted and therefore, they can serve as**  
42 **benchmark solutions.**  
43  
44

45  
46 The paper is organised as follows. Section 2.1 reviews briefly the general  
47 framework and some properties of the spectral dynamic stiffness method (SDSM)  
48 developed in [27–29]. The spectral dynamic stiffness theory for non-uniform elas-  
49 tic supports and mass attachments is then presented in Section 2.2.1, which is fol-  
50 lowed by that for non-uniform elastic coupling constraints, see Section 2.2.2. **The**  
51 **current SDS theory can also be degenerated and applied to the classical DSM, see**  
52  
53  
54  
55  
56  
57  
58

1  
2  
3  
4  
5 **Section 2.2.3.** In Section 3.1, investigations on convergence and computational  
6 efficiency are carried out and the SDSM results are validated by published results.  
7 From Sections 3.2 to 3.3, three practical problems in different engineering areas  
8 are illustrated. Finally, significant conclusions are drawn in Section 4.  
9

## 10 11 12 **2. Theory**

13  
14 In essence, the purpose of this paper is to substantially extend a recently de-  
15 veloped spectral dynamic stiffness method (SDSM) [27–29] to more general and  
16 diversified cases. Therefore, the basic framework and properties of the SDSM are  
17 briefly summarised below to provide the necessary background for the SDS devel-  
18 opment for arbitrary non-uniform elastic supports, mass attachments and elastic  
19 coupling constraints.  
20  
21

### 22 *2.1. The Spectral Dynamic Stiffness Method (SDSM)*

#### 23 *2.1.1. Framework of the SDSM*

24  
25 The SDSM [27–29] combines the spectral (S) method and the classical dy-  
26 namic stiffness method (DSM). One of the key points in the SDSM lies in adopting  
27 a modified Fourier series [30]. The adopted modified Fourier series for any arbi-  
28 trary displacement or force boundary condition (denoted by  $h(\xi)$ ) along a plate  
29 edge (line node  $\xi \in [-L, L]$  in local coordinates of plate) is given by  
30  
31

$$32  
33 h(\xi) = \sum_{\substack{s \in \mathbb{N} \\ l \in \{0,1\}}} H_{ls} \frac{\mathcal{T}_l(\gamma_{ls}\xi)}{\sqrt{\zeta_{ls}L}}, \quad H_{ls} = \int_{-L}^L h(\xi) \frac{\mathcal{T}_l(\gamma_{ls}\xi)}{\sqrt{\zeta_{ls}L}} d\xi, \quad (1)$$

34  
35 where  $\mathbb{N} = \{0, 1, 2, \dots\}$  is the non-negative integer set, and the subscript ‘ $l$ ’, taking  
36 value of either ‘0’ or ‘1’, denotes the corresponding symmetric or antisymmetric  
37 functions (and coefficients). Here,  $\zeta_{ls}$  is given as  
38  
39  
40  
41

$$42  
43 \zeta_{ls} = \begin{cases} 2 & l = 0 \text{ and } s = 0 \\ 1 & l = 1 \text{ or } s \geq 1 \end{cases}. \quad (2)$$

44  
45 The corresponding modified Fourier basis function  $\mathcal{T}_l(\gamma_{ls}\xi)$  in Eq. (1) is defined  
46 as  
47

$$48  
49 \mathcal{T}_l(\gamma_{ls}\xi) = \begin{cases} \cos(\frac{s\pi}{L}\xi) & l = 0 \\ \sin((s + \frac{1}{2})\frac{\pi}{L}\xi) & l = 1 \end{cases}, \quad \xi \in [-L, L], \quad s \in \mathbb{N}, \quad (3)$$

50  
51 which provides a complete and orthogonal set to described any one-dimensional  
52 function  $h(\xi)$  of Eq. (1) with any arbitrary boundary conditions. It should be  
53 emphasised that the above modified Fourier series has strong orthogonality which  
54 is one of the most important factors that makes the SDSM numerically stable  
55  
56  
57  
58  
59  
60  
61  
62  
63  
64  
65

with no precondition, therefore any higher order of modified Fourier series can be adopted in the computation to compute results within any desired accuracy. The  $\sqrt{\zeta_{ls}L}$  appearing in Eq. (1) provides the symmetry of the forward and inverse Fourier transformation. These above techniques are used for the purpose of retaining the symplecticity [37] of the formulated system. It will be shown later that the modified Fourier series of Eq. (1) also benefits the conciseness of the theory presented in this paper.

By using the above modified Fourier series, the general solution of the governing differential equation (GDE) for isotropic [27] or composite [28] plate elements with arbitrary boundary conditions in the frequency domain can be achieved. In the next step, the SDS matrix for the plate element can be analytically formulated by substituting the above general solution into the general boundary conditions (BC) by some algebraic manipulation. Indeed, the analytical expressions involved in the SDSM are concise but can be used to handle complex plate-like structures with any arbitrary boundary conditions [27–29].

Next, the analytically expressed spectral dynamic stiffness (SDS) matrix of the plate element can be assembled directly to model complex plate-like structures. The assembly procedure is similar to that of the finite element (FE) method with the exception that the FE elements are generally connected at point nodes whereas the SDS plate elements are connected on *line nodes*. Here the line nodes represent either the plate boundaries and/or the inter-element edges which have the flexibility to describe any arbitrary BC or continuity conditions (CC). In general, for a plate assembly, the analytical SDSM formulation can be written in the following form

$$\mathbf{f} = \mathbf{K}\mathbf{d}, \quad (4)$$

where  $\mathbf{K}$  is the SDS matrix of the complete plate assembly, which relates the modified Fourier coefficient vector of the force  $\mathbf{f}$  to that of the displacement  $\mathbf{d}$  on all of the line nodes (boundaries and inter-element edges) of the plate assembly, so that

$$\mathbf{f} = [\mathbf{f}_1^T, \mathbf{f}_2^T, \dots, \mathbf{f}_i^T, \dots, \mathbf{f}_{N_{lDOF}}^T]^T, \quad \mathbf{d} = [\mathbf{d}_1^T, \mathbf{d}_2^T, \dots, \mathbf{d}_i^T, \dots, \mathbf{d}_{N_{lDOF}}^T]^T. \quad (5)$$

In Eq. (5), the subscript  $N_{lDOF}$  is the total number of *line degrees of freedom (line DOF)* of the plate assembly (Theoretically, each *line DOF* has infinite DOF since each BC function is a continuous function on  $\xi \in [-L, L]$ ). Here,  $N_{lDOF} = ln \times N_{lDOF}$  where  $ln$  is the number of total *line nodes* of the plate assembly whereas  $N_{lDOF}$  represents the number of *line DOF* of each line node (for instance, an individual rectangular Kirchhoff plate, being a special case of the plate assembly, has four edges, i.e.,  $ln = 4$  and each edge has two *line DOF*  $W$  and  $\phi$ , i.e.,  $N_{lDOF} = 2$ ). Each force  $\mathbf{f}_i$  and displacement  $\mathbf{d}_i$  sub-vectors in Eq. (5) take the

following form

$$\mathbf{f}_i = [F_{i00}, F_{i01}, F_{i02}, \dots, F_{i10}, F_{i11}, F_{i12}, \dots]^T, \quad (6a)$$

$$\mathbf{d}_i = [D_{i00}, D_{i01}, D_{i02}, \dots, D_{i10}, D_{i11}, D_{i12}, \dots]^T, \quad (6b)$$

where  $F_{ils}$  and  $D_{ils}$  ( $l \in \{0, 1\}, s \in \mathbb{N}$ ) are respectively the modified Fourier coefficients of the corresponding force  $f_i(\xi)$  and displacement  $d_i(\xi)$  BC (or CC) applied on the  $i$ th line DOF of the plate assembly, which are obtained by applying Eq. (1) onto  $f_i(\xi)$  and  $d_i(\xi)$  respectively to give

$$F_{ils} = \int_{-L}^L f_i(\xi) \frac{\mathcal{T}_l(\gamma_{ls}\xi)}{\sqrt{\zeta_{ls}L}} d\xi, \quad (7a)$$

$$D_{ils} = \int_{-L}^L d_i(\xi) \frac{\mathcal{T}_l(\gamma_{ls}\xi)}{\sqrt{\zeta_{ls}L}} d\xi. \quad (7b)$$

Therefore, each term of either  $F_{ils}$  or  $D_{ils}$  in Eq. (7) represents a frequency-wavenumber dependent DOF (FWDOF) of the  $i$ th line DOF. Following the definitions given in Eqs. (1) to (3), the subscript ‘ $l$ ’ in Eq. (7), being ‘0’ or ‘1’, stands respectively for the modified Fourier cosine (for symmetric component) or sine (for antisymmetric component) coefficients of the  $i$ th line DOF. Therefore, the BC (or CC) can be arbitrarily prescribed along any line DOF, which are directly transformed through Eq. (7) into vector form (i.e.,  $\mathbf{f}_i$  and  $\mathbf{d}_i$ ) of Eq. (6) and eventually into  $\mathbf{f}$  and  $\mathbf{d}$  in Eq. (5). For example, when the Kirchhoff plate theory for composite plate elements is utilised, the general BC is given as [28]

$$\left. \begin{aligned} \delta W : \quad & V_x = -D_{11} \left( \frac{\partial^3 W}{\partial x^3} + (2\Gamma - \nu_{21}) \frac{\partial^3 W}{\partial x \partial y^2} + \chi \frac{\partial W}{\partial x} \right) \\ \delta \phi_x = -\delta \frac{\partial W}{\partial x} : \quad & M_{xx} = -D_{11} \left( \frac{\partial^2 W}{\partial x^2} + \nu_{21} \frac{\partial^2 W}{\partial y^2} \right) \end{aligned} \right\} \text{for } x \pm a, \quad (8a)$$

$$\left. \begin{aligned} \delta W : \quad & V_y = -D_{11} \left( \Lambda \frac{\partial^3 W}{\partial y^3} + (2\Gamma - \nu_{21}) \frac{\partial^3 W}{\partial y \partial x^2} + \chi \frac{\partial W}{\partial y} \right) \\ \delta \phi_y = -\delta \frac{\partial W}{\partial y} : \quad & M_{yy} = -D_{11} \left( \Lambda \frac{\partial^2 W}{\partial y^2} + \nu_{21} \frac{\partial^2 W}{\partial x^2} \right) \end{aligned} \right\} \text{for } y = \pm b, \quad (8b)$$

where  $\Gamma = (D_{12} + 2D_{66})/D_{11}$ ,  $\Lambda = D_{22}/D_{11}$ ,  $\chi = \omega^2 I_2/D_{11}$ . Note that  $D_{ij}$  denotes the bending stiffness of the plate in the classical laminate theory [38],  $I_2$  is the rotatory inertia of the related plate edges and  $\omega$  is the angular frequency, see [28]. In this case,  $f_i(\xi)$  of Eq. (7a) represents either  $V$  ( $V_x$  or  $V_y$ ) or  $M$  ( $M_{xx}$  or  $M_{yy}$ ) of Eq. (8) whereas  $d_i(\xi)$  of Eq. (7b) denotes either  $W$  or  $\phi$  ( $\phi_x$  or  $\phi_y$ ) of Eq. (8) on the corresponding boundary or inter-element edges.

### 2.1.2. Some important properties of the SDSM

Some important properties of the SDSM [27–29] are summarised as follows:

- **Exactness:** The SDSM should be regarded as an exact series-based method which converges to exact results with an exceptionally fast convergence rate [27, 29]. This is because the formulation satisfies exactly the GDE of plate motion and any arbitrary BC are satisfied in an exact series sense. Moreover, unlike most other analytical methods, the SDSM is unconditionally numerically stable for any higher order series terms, allowing the method to compute results within any desired accuracy.
- **Efficiency:** The SDSM is highly efficient mainly due to the fact that it uses a very small number of DOF which, nevertheless, represent the structure most accurately. This is because the spectral dynamic stiffness (SDS) matrix is formulated on the line nodes (similar to the boundary element method), and represents the system in a spectral sense. Moreover, the enhancements of the Wittrick-Williams algorithm where the so-called  $J_m$  problem has been elegantly resolved to allow modelling of complex plate structures with as few elements as possible.
- **Robustness:** The SDSM computes any required natural frequencies of plate-like structures covering from low to high frequency ranges. There is no possibility of missing any natural frequencies and no spurious frequencies will be unnecessarily captured. This is also due to the application of the enhanced Wittrick-Williams algorithm.
- **Versatility:** The SDSM can be assembled as easily as the finite element method. Clearly, the SDSM can handle not only a single plate but also complex plate-like structures made of isotropic as well as composite materials which can be subjected to any arbitrary boundary conditions [27–29].

In this paper, all of the above advantages of the SDSM will be retained and yet the versatility of the SDSM will be significantly extended. Any arbitrary non-uniformly distributed elastic supports, mass attachments as well as elastic coupling constraints (illustrated in Fig. 1) along any of the line nodes are successfully incorporated following a similar *spectral* framework of that of the SDSM. The developed SDS matrices for the above three general types of non-uniform BC and/or CC are directly superposed onto that of a complete plate assembly.

## 2.2. SDS formulation for non-uniform elastic supports, mass attachments and coupling constraints

In this section, an SDS theory is developed for arbitrary non-uniform elastic supports and mass attachments along any of the line nodes (Section 2.2.1) as well as for any arbitrary non-uniform elastic coupling constraints applied between any two line nodes (Section 2.2.2). **The developed SDS theory can also be applied to classical dynamic stiffness method which is described in Section 2.2.3.**

### 2.2.1. Development of the SDS matrices for non-uniform elastic supports and mass attachments

The SDS theory for non-uniform elastic supports (Fig.1(a)) and mass attachments (Fig. 1(b)) is developed with the basic premise that the Kirchhoff plate theory is applied. (Of course, the same procedure is applicable to other SDS elements such as those for plane elasticity [31].) Based on the Kirchhoff plate theory (recalling Eq. (8)), there are generally two types of *generalised displacements* along each plate line node (either boundary or inter-element edge), namely, the translational displacement  $W(\xi)$ ; and the bending rotation  $\phi(\xi)$  and the corresponding two *generalised forces* are the effective transverse shear force  $V(\xi)$  and bending moment  $M(\xi)$  respectively. For notational convenience,  $\xi$  is used in this paper to represent  $x$  or  $y$  which appears in Eq. (8). Therefore,  $\xi \in [-L, L]$  with  $L$  denoting  $a$  or  $b$  respectively. The elastic supports and/or mass attachments applied on a certain *line DOF* of a plate assembly will give rise to additional dynamic stiffness contribution onto this line DOF during the vibratory motion. The additional generalised boundary forces (superscripted by ‘ $a$ ’) induced by the elastic supports and mass attachments can be written in the following form

$$V^a(\xi) = K_w(\xi)W(\xi), \quad V^a(\xi) = -\omega^2 m(\xi)W(\xi), \quad (9a)$$

$$M^a(\xi) = K_\phi(\xi)\phi(\xi), \quad M^a(\xi) = -\omega^2 I_2(\xi)\phi(\xi), \quad (9b)$$

where  $K_w(\xi)$  and  $K_\phi(\xi)$  are the translational and rotational stiffnesses of the elastic supports along the line node  $\xi \in [-L, L]$  (see Fig. 1(a)), whereas  $m(\xi)$  and  $I_2(\xi)$  are the mass and rotatory inertia distribution of the attached line mass (see Fig. 1(b), and  $\omega$  is the angular frequency). All functions  $K_w(\xi)$ ,  $K_\phi(\xi)$ ,  $m(\xi)$  and  $I_2(\xi)$  can be arbitrarily specified on  $\xi \in [-L, L]$ , which can of course, be either uniformly or non-uniformly distributed. They can be prescribed either in an analytical or in a numerical manner (appropriate discrete form of modified Fourier series formula corresponding to Eq. (1) can be used). For notational convenience, the above two *generalised displacements*  $W(\xi)$  and  $\phi(\xi)$  in Eq. (9) are denoted by  $d_i(\xi)$  whereas the two additional *generalised forces*  $V^a(\xi)$  and  $M^a(\xi)$  are represented by  $f_i^a(\xi)$ , where the subscript  $i$  denotes the  $i$ th line DOF on which the non-uniform elastic support or mass attachment is applied. Therefore, the four equations in Eq. (9) can be expressed in a unified form as

$$f_i^a(\xi) = \mu G^a(\xi)d_i(\xi), \quad \xi \in [-L, L], \quad (10)$$

where  $\mu G^a(\xi)$  represents one of the four non-uniform distributions in Eq. (9), namely,  $K_w(\xi)$ ,  $K_\phi(\xi)$ ,  $-\omega^2 m(\xi)$  and  $-\omega^2 I_2(\xi)$  which are applied onto the  $i$ th line DOF.  $G^a(\xi)$  is a *dimensionless distribution function* and  $\mu$  is the *stiffness or mass dynamic stiffness constant* which represents one of the four constants:

Table 1: Dimensional analysis and the dimensionless form of the stiffness or mass constants related to  $\mu$  of Eq. (10).  $D$  stands for the plate bending rigidity,  $L_b$  denotes the length of the corresponding line node, which equals to  $2L$  for  $\xi \in [-L, L]$ ;  $m_p$  is the total mass of the parent plate structure.

	$K_{w0}$	$K_{\phi_0}$	$m_0$	$I_{20}$
Dimensional analysis*	$[\hat{M}][\hat{L}]^{-1}[\hat{T}]^{-2}$	$[\hat{M}][\hat{L}][\hat{T}]^{-2}$	$[\hat{M}][\hat{L}]^{-1}$	$[\hat{M}][\hat{L}]$
Dimensionless form	$\frac{K_{w0}L_b^3}{D}$	$\frac{K_{\phi_0}L_b}{D}$	$\frac{m_0L_b}{m_p}$	$\frac{I_{20}}{m_pL_b}$

\*  $[\hat{M}]$ ,  $[\hat{L}]$  and  $[\hat{T}]$  represent respectively the mass, length and time in dimensional analysis.

$K_{w0}$ ,  $K_{\phi_0}$  or  $-\omega^2 m_0$ ,  $-\omega^2 I_{20}$ . The dimensional analysis and the corresponding dimensionless form for  $K_{w0}$ ,  $K_{\phi_0}$ ,  $m_0$  and  $I_{20}$  are illustrated in Table 1.

In what follows, the development of the SDS matrices for arbitrarily distributed elastic supports and mass attachments are presented. By recalling the essence of the SDSM as indicated in Eqs. (4) to (7),  $\mathbf{f}_i$  and  $\mathbf{d}_i$  are the modified Fourier series coefficient vectors of the generalised force and displacement BC (or CC) of the  $i$ th line DOF. Note that  $\mathbf{f}_i$  and  $\mathbf{d}_i$  are related by the corresponding component  $\mathbf{K}_{ii}$  of the SDS matrix  $\mathbf{K}$  given by Eq. (4) without considering elastic supports or mass attachments. Therefore,  $\mathbf{K}_{ii}$  provides a linear mapping among the generalised force and displacement corresponding to all FWDOF of the  $i$ th line DOF. Next, additional SDS matrices of the elastic supports and mass attachments  $\mathbf{K}_{ii}^a$  are formulated following the steps given below which eventually will be superposed to  $\mathbf{K}_{ii}$ .

First, expressing the generalised displacement  $d_i(\xi)$  in terms of the modified Fourier series of Eq. (1) (using the notation  $l, s$  for  $d_i(\xi)$ ), Eq. (10) becomes

$$f_i^a(\xi) = \mu G^a(\xi) \sum_{\substack{s \in \mathbb{N} \\ l \in \{0,1\}}} \left[ D_{ils} \frac{\mathcal{T}_l(\gamma_{ls}\xi)}{\sqrt{\zeta_{ls}L}} \right], \quad (11)$$

where  $D_{ils}$ , already given by Eq. (7b), represents the displacement component for each FWDOF of the  $i$ th line DOF. Then, applying the modified Fourier series of Eq. (7a) (using the notation  $t, r$  for  $f_i^a(\xi)$ ) to distinguish with the previous  $l, s$  for  $d_i(\xi)$ ) to both sides of Eq. (11), one has

$$F_{tr}^a = \mu \int_{-L}^L G^a(\xi) \sum_{\substack{s \in \mathbb{N} \\ l \in \{0,1\}}} \left[ D_{ils} \frac{\mathcal{T}_l(\gamma_{ls}\xi)}{\sqrt{\zeta_{ls}L}} \right] \frac{\mathcal{T}_t(\gamma_{tr}\xi)}{\sqrt{\zeta_{tr}L}} d\xi, \quad (\forall) t \in \{0, 1\}, r \in \mathbb{N}. \quad (12)$$

Here,  $F_{tr}^a$  denotes the additional force component related to each FWDOF in the same form as Eq. (6a) which is generated by the non-uniform elastic supports or

mass attachments given by  $\mu G^a(\xi)$ . Therefore, one can obtain the additional force vector  $\mathbf{f}_i^a$  caused by the elastic support or mass attachment along the  $i$ th line DOF in the form

$$\mathbf{f}_i^a = \mathbf{K}_{ii}^a \mathbf{d}_i = \mu \mathbf{G}^a \mathbf{d}_i, \quad (13)$$

where  $\mathbf{K}_{ii}^a = \mu \mathbf{G}^a$  is the SDS matrix for the applied elastic support or mass attachment. Based on Eq. (12), the *dimensionless SDS matrix*  $\mathbf{G}^a$  should be symmetric and can be generally expressed in the following form

$$\mathbf{G}^a = \begin{bmatrix} \mathbf{G}_{00}^a & \mathbf{G}_{01}^a \\ \mathbf{G}_{10}^a & \mathbf{G}_{11}^a \end{bmatrix}. \quad (14)$$

The four sub-matrices  $\mathbf{G}_{tl}^a$  (with  $t, l \in \{0, 1\}$ ) are  $S \times S$  matrices if  $S$  terms are adopted in the modified Fourier series, namely,  $s, r \in [0, S - 1]$  for Eq. (12). ( $S$  coincides with  $M$  or  $N$  where  $M$  and  $N$  are the numbers of terms adopted in the series for the related plate element in the  $x$  and  $y$  directions respectively, see [27, 28].) The analytical expressions for the entries of  $\mathbf{G}_{tl}^a$  are derived analytically from Eq. (12) which takes the following concise form

$$\mathbf{G}_{tl}^a(r, s) = \frac{1}{\sqrt{\zeta_{tr}\zeta_{ts}}L} \int_{-L}^L G^a(\xi) \mathcal{T}_l(\gamma_{ts}\xi) \mathcal{T}_t(\gamma_{tr}\xi) d\xi. \quad (15)$$

Therefore, once any arbitrary dimensionless distribution function  $G^a(\xi)$  is given, the analytical expressions for the corresponding matrix  $\mathbf{G}^a$  can be derived using the above concise equation. The integration in Eq. (15) can be preformed straightforwardly either by symbolic software like MATHEMATICA or by hand. The analytical expressions for  $\mathbf{G}^a$  matrices corresponding to several typical distribution functions  $G^a(\xi)$  are given in Appendix A. For any arbitrary distribution function  $\widetilde{G}^a(\xi)$  which can be expressed as the superposition of the known functions  $G^a(\xi)$ , the corresponding dimensionless SDS matrix  $\widetilde{\mathbf{G}}^a$  can be formulated easily by summing up the known  $\mathbf{G}^a$  matrices multiplied by the corresponding coefficients. For example, if the dimensionless distribution function  $\widetilde{G}^a(\xi)$  applied onto the  $i$ th line DOF is given as:  $\widetilde{G}^a(\xi) = k_0 + k_1(\xi/L) + k_2(\xi/L)^2 + k_{cos} \cos(\pi\xi/(2L))$  where  $k_0, k_1, k_2$  and  $k_{cos}$  can take any constant values, then the corresponding dimensionless SDS matrix is simply formulated as  $\widetilde{\mathbf{G}}^a = k_0 \mathbf{G}_0^a + k_1 \mathbf{G}_1^a + k_2 \mathbf{G}_2^a + k_{cos} \mathbf{G}_{cos}^a$ . Here,  $\mathbf{G}_0^a, \mathbf{G}_1^a, \mathbf{G}_2^a$  and  $\mathbf{G}_{cos}^a$  are respectively the dimensionless SDS matrices for 1,  $\xi/L, (\xi/L)^2$  and  $\cos(\pi\xi/(2L))$  as given in Appendix A, which are derived by using Eqs. (14) and (15). It should be noted that there are two special cases for the dimensionless distribution function when  $G^a(\xi)$  can be either an even (symmetric) or an odd (antisymmetric) function for  $\xi \in [-L, L]$ . When  $G^a(\xi)$  is an even function, Eq. (14) will have  $\mathbf{G}_{01}^a = \mathbf{G}_{10}^a = \mathbf{O}$  whereas  $\mathbf{G}_{00}^a$  and  $\mathbf{G}_{11}^a$  are obtained from Eq. (15). When  $G^a(\xi)$  is an odd function, Eq. (14) will have  $\mathbf{G}_{00}^a = \mathbf{G}_{11}^a = \mathbf{O}$  whereas  $\mathbf{G}_{01}^a$  and  $\mathbf{G}_{10}^a$  are obtained from Eq. (15).

1  
2  
3  
4  
5 The SDS matrix  $\mathbf{K}_{ii}^a = \mu \mathbf{G}^a$  developed above for the elastic support or mass  
6 attachment along the  $i$ th line DOF is eventually superposed to the SDS matrix  
7 component  $\mathbf{K}_{ii}$  to form the  $ii$  component of the final SDS matrix of the plate  
8 assembly  $\mathbf{K}^{final}$  considering those supports and attachments to arrive at  
9

$$10 \quad \mathbf{K}_{ii}^{final} = \mathbf{K}_{ii} + \mu \mathbf{G}^a. \quad (16)$$

### 11 12 13 2.2.2. Development of the SDS matrices for non-uniform elastic coupling con- 14 straints 15

16 The procedure in the last section can be adapted for non-uniformly elastically  
17 coupled line DOF, see Fig. 1(c). This type of boundary and/or continuity con-  
18 ditions (BC and/or CC) have very important practical applications as mentioned  
19 earlier in the Introduction, and whose SDS formulation is also accomplished in a  
20 concise manner.  
21

22 Let us assume that the  $i$ th and the  $j$ th line DOF (along either boundaries  
23 or inter-element edges) of a plate assembly are elastically coupled with non-  
24 uniformly distributed coupling stiffness  $C(\xi)$ . In Kirchhoff plate theory for ex-  
25 ample,  $C(\xi)$  stands for either translational coupling stiffness  $C_w(\xi)$  or rotational  
26 coupling stiffness  $C_\phi(\xi)$ , see Fig. 1(c). The coupling equation will then become  
27  
28

$$29 \quad C(\xi) [d_i(\xi) - d_j(\xi)] = f_i^a(\xi) = -f_j^a(\xi), \quad \xi \in [-L, L], \quad (17)$$

30 where  $d_i(\xi)$  and  $d_j(\xi)$  are the generalised displacements for the  $i$ th and  $j$ th line  
31 DOF respectively;  $f_i^a(\xi)$  and  $f_j^a(\xi)$  are the additional coupling forces acting on  
32 the corresponding line DOF due to the coupling constraint  $C(\xi)$ . Therefore, Eq.  
33 (17) can be rewritten in the following matrix form  
34  
35  
36  
37

$$38 \quad \begin{bmatrix} f_i^a(\xi) \\ f_j^a(\xi) \end{bmatrix} = \begin{bmatrix} C(\xi) & -C(\xi) \\ -C(\xi) & C(\xi) \end{bmatrix} \begin{bmatrix} d_i(\xi) \\ d_j(\xi) \end{bmatrix}, \quad \xi \in [-L, L]. \quad (18)$$

39 Similar to Eq. (10), the above coupling constraint stiffness function  $C(\xi)$  can  
40 also be written in the form  
41  
42  
43

$$44 \quad C(\xi) = \mu G^a(\xi), \quad (19)$$

45 where  $\mu$  is the coupling dynamic stiffness constant similar to the  $\mu$  described in  
46 Section 2.2.1, and  $G^a(\xi)$  is again, the dimensionless distribution function. There-  
47 fore, the first few steps of the SDS formulation for a non-uniform coupling con-  
48 straint follow the same procedure for the previous elastic supports and mass at-  
49 tachments as described in Eqs. (10) through (12). The main difference that will  
50 show up afterwards is that the forces of the two elastically coupled line DOF are  
51 related to the two displacements as illustrated in Eq. (18). Consequently, the  
52  
53  
54  
55  
56  
57  
58  
59  
60  
61  
62  
63  
64  
65

1  
2  
3  
4  
5 SDS matrix of a non-uniform elastic coupling constraint  $C(\xi) = \mu G^a(\xi)$  for the  
6 elastically coupled two edges can be written in the form  
7

$$8 \quad \begin{bmatrix} \mathbf{f}_i^a \\ \mathbf{f}_j^a \end{bmatrix} = \mu \begin{bmatrix} \mathbf{G}^a & -\mathbf{G}^a \\ -\mathbf{G}^a & \mathbf{G}^a \end{bmatrix} \begin{bmatrix} \mathbf{d}_i \\ \mathbf{d}_j \end{bmatrix}, \quad (20)$$

9  
10  
11 where matrix  $\mathbf{G}^a$  is the same as that of Eq. (14) but corresponds to the elastic  
12 coupling stiffness distribution function  $G^a(\xi)$  given in Eq. (19). Next, the sub-  
13 SDS matrices  $\mu \mathbf{G}^a$  in Eq. (20) are superposed directly to the FWDOF (rows and  
14 columns) corresponding to the  $i$ th and  $j$ th line DOF of the SDS matrix for the  
15 plate assembly resulting in  
16  
17

$$18 \quad \begin{aligned} 19 \quad \mathbf{K}_{ii}^{final} &= \mathbf{K}_{ii} + \mu \mathbf{G}^a, & \mathbf{K}_{jj}^{final} &= \mathbf{K}_{jj} + \mu \mathbf{G}^a, \\ 20 \quad \mathbf{K}_{ij}^{final} &= \mathbf{K}_{ij} - \mu \mathbf{G}^a, & \mathbf{K}_{ji}^{final} &= \mathbf{K}_{ji} - \mu \mathbf{G}^a. \end{aligned} \quad (21)$$

21  
22 Repeating the procedure described in Sections 2.2.1 and 2.2.2 and follow-  
23 ing Eqs. (16) and (21) for each elastic supports, mass attachments and elastic  
24 coupling constraints, the final SDS matrix of the complete structure is formul-  
25 ated. Next, any arbitrarily prescribed classical boundary conditions are applied  
26 following the same procedure described in Section 2.1.1 (for more details are re-  
27 ferred to [28]). Finally, an enhanced Wittrick-William algorithm [28] is applied  
28 to obtain any required natural frequencies to any desired accuracy for the plate-  
29 support/attachment/constraint system.  
30  
31

32 It is worth emphasising that in both Sections 2.2.1 and 2.2.2, the stiffnesses  
33  $K_w(\xi)$ ,  $K_\phi(\xi)$  and  $C_w(\xi)$ ,  $C_\phi(\xi)$  can be given sufficiently large values to act as  
34 penalty parameters to model respectively the corresponding fixed line DOFs and  
35 rigidly connected line DOFs. This is fairly straightforward to apply and has been  
36 used in a lot of existing work in the literature, see for example, [18, 26]. However,  
37 this penalty method has some drawbacks. When applied to non-uniform elastic  
38 support and coupling constraints, the main drawback lies in the difficulty in deter-  
39 mining a suitable magnitude for the penalty parameters, i.e., too small will lead  
40 to loss of accuracy; too large may cause ill-conditioning or large round off errors  
41 [28]. In the current SDS theory, the penalty method is not used to ensure that  
42 the results are completely reliable and therefore exact solutions are confidentially  
43 achieved. In the current theory, the fixed supports are exactly represented by zero  
44 displacement for all the FWDOF of the fixed line DOFs, and rigidly connected line  
45 DOFs with the same  $W(\xi)$  or  $\phi(\xi)$  are exactly represented by shared FWDOF for  
46 the related displacement ( $W(\xi)$  and/or  $\phi(\xi)$ ) along the coupled edges.  
47  
48  
49  
50  
51  
52

### 53 *2.2.3. Application of the current SDS theory to the classical DSM*

54 **Significant contributions have recently been reported by developing the clas-**  
55 **sical DSM to generate various dynamic stiffness (DS) elements [32–36] using**  
56  
57  
58

1  
2  
3  
4  
5 refined theories (e.g., Carrera’s Unified formulation). The current theory pre-  
6 sented in Sections 2.2.1 and 2.2.2 can be degenerated, as a special case, to be  
7 applied to such DS elements with *uniform* elastic supports, mass attachments and  
8 elastic coupling constraints. Naturally, Eqs. (16) and (21) still apply but with  
9 the dimensionless matrix  $\mathbf{G}^a$  reduced to the unit scalar 1 whereas  $\mu$  represents  
10 the corresponding *stiffness*, or *mass*, or *coupling dynamic stiffness constants* of  
11 the *uniform* elastic supports, or mass attachments, or elastic coupling constraints,  
12 respectively.  
13

14  
15 However, it should be noted that the capability of modelling non-uniform elas-  
16 tic supports and/or mass attachments and/or coupling constraints has been made  
17 possible only within the framework of the SDSM [27–29, 31]. The classical DS  
18 elements in [32–35] can not be used to model plates with non-uniform BC and/or  
19 CC described in this paper. This is because the DSM is essentially based on the  
20 assumption that the deformation of the plate in one direction is essentially a sin-  
21 gle sine function *in prior*, which is valid only for plate elements with opposite  
22 edges simply supported. Moreover, the formulation can handle only uniformly  
23 distributed elastic supports mass attachments and coupling constraints. Relevant,  
24 but more detailed interpretation on this matter is given in [27]. In order to treat the  
25 non-uniform BC and/or CC, ‘spectral’ concept should be necessarily introduced,  
26 and then the theory of this paper can be fruitfully applied.  
27  
28  
29  
30  
31

### 32 **3. Results and applications**

33  
34 The theory developed above is implemented in a MATLAB program which  
35 computes exact natural frequencies and mode shapes of plates and plates assem-  
36 blies with arbitrarily distributed elastic supports and/or mass attachments and/or  
37 elastic coupling constraints. In Section 3.1, the convergence and computational  
38 efficiency analyses are performed, and then the current SDS theory is validated  
39 by published results from the literature. Next, three practical composite plate-like  
40 structures are analysed and results are given in Sections 3.2 to 3.4. Note that all  
41 SDSM results (shown in bold) are accurate up to the last significant figure and  
42 therefore, will serve as benchmark solutions. It should be kept in mind that the  
43 dimensions of all single plates in Tables 2 to 5 are denoted in the form of  $2a \times 2b$   
44 instead of  $a \times b$ , and the dimensionless frequency parameters are defined accord-  
45 ingly.  
46  
47  
48  
49

#### 50 *3.1. Convergence, computational efficiency and validation*

51  
52 In the numerical implementation of the SDS theory, the infinite algebraic ma-  
53 trix  $\mathbf{G}^a$  for any non-uniform elastic supports and/or mass attachments and/or elas-  
54 tic coupling constraints will have to be eventually truncated at a certain stage  
55 during computation. This procedure is the same as that of the  $\mathbf{K}$  matrix for plate  
56  
57  
58  
59  
60  
61  
62  
63  
64  
65

assemblies as described in Section 2.1.1 (more details can be found in [27–29]). Therefore, it is important to examine the convergence rate of the method. To this end, it will be shown that the SDSM for plate assemblies with non-uniform elastic constraints and/or mass attachments and/or elastic coupling constraints has excellent convergence rate and computational efficiency.

Table 2: Convergence and computational efficiency studies for a square isotropic plate ( $2a \times 2b = 2L \times 2L$  and  $\nu = 0.3$ ) with four different cases with parabolic elastic supports whose translational and rotational stiffnesses are  $K_w(\xi) = D/(2a)^3[1 - (\xi/L)^2]/4$  and  $K_\phi(\xi) = D/(2a)[1 - (\xi/L)^2]/4$ , respectively.

BC	$M = N$	$\lambda = 4\omega a^2 \sqrt{\rho h/D}$								Time (s)
		1	2	3	4	5	6	7	8	
CE <sub>φ</sub> CE <sub>φ</sub>	3	29.1002	55.0496	69.3747	94.7113	102.525	129.056	140.252	154.599	0.29
	5	29.1025	55.0628	69.3818	94.7441	102.599	129.122	140.439	154.860	0.33
	10	<b>29.1026</b>	<b>55.0634</b>	<b>69.3821</b>	<b>94.7459</b>	<b>102.602</b>	<b>129.123</b>	<b>140.446</b>	<b>154.869</b>	0.46
E <sub>φ</sub> CSC	15	<b>29.1026</b>	<b>55.0634</b>	<b>69.3821</b>	<b>94.7459</b>	<b>102.602</b>	<b>129.123</b>	<b>140.446</b>	<b>154.869</b>	0.74
	3	29.0239	54.8891	69.3469	94.6305	102.332	129.041	140.130	154.551	0.28
	5	29.0263	54.9026	69.3542	94.6637	102.406	129.108	140.318	154.814	0.34
EEEE	10	<b>29.0264</b>	<b>54.9032</b>	<b>69.3545</b>	<b>94.6655</b>	<b>102.409</b>	<b>129.109</b>	<b>140.325</b>	<b>154.822</b>	0.47
	15	<b>29.0264</b>	<b>54.9032</b>	<b>69.3545</b>	<b>94.6655</b>	<b>102.409</b>	<b>129.109</b>	<b>140.325</b>	<b>154.822</b>	0.72
	2	0.815915	2.23858	2.23858	13.6452	20.5188	24.7266	35.1475	35.1475	0.21
E <sub>w</sub> E <sub>w</sub> E <sub>w</sub> E <sub>w</sub>	5	0.815930	2.23741	2.23741	13.6437	20.5187	24.7238	35.1394	35.1394	0.29
	10	<b>0.815931</b>	<b>2.23734</b>	<b>2.23734</b>	<b>13.6436</b>	<b>20.5186</b>	<b>24.7238</b>	<b>35.1392</b>	<b>35.1392</b>	0.44
	15	<b>0.815931</b>	<b>2.23734</b>	<b>2.23734</b>	<b>13.6436</b>	<b>20.5186</b>	<b>24.7238</b>	<b>35.1392</b>	<b>35.1392</b>	0.76
E <sub>w</sub> E <sub>w</sub> E <sub>w</sub> E <sub>w</sub>	2	<b>0.816380</b>	<b>9.91502</b>	<b>9.91502</b>	<b>19.7627</b>	<b>39.4856</b>	<b>39.4959</b>	<b>49.3590</b>	<b>49.3590</b>	0.20
	5	<b>0.816380</b>	<b>9.91502</b>	<b>9.91502</b>	<b>19.7627</b>	<b>39.4856</b>	<b>39.4959</b>	<b>49.3590</b>	<b>49.3590</b>	0.26
	10	<b>0.816380</b>	<b>9.91502</b>	<b>9.91502</b>	<b>19.7627</b>	<b>39.4856</b>	<b>39.4959</b>	<b>49.3590</b>	<b>49.3590</b>	0.39
	15	<b>0.816380</b>	<b>9.91502</b>	<b>9.91502</b>	<b>19.7627</b>	<b>39.4856</b>	<b>39.4959</b>	<b>49.3590</b>	<b>49.3590</b>	0.62

At first, the convergence and computational efficiency investigation for the current method is carried out for four representative cases of a square isotropic plate ( $2a \times 2b = 2L \times 2L$  and  $\nu = 0.3$ ) with different combinations of parabolic elastic and classical boundary conditions. The four cases studied are: CE<sub>φ</sub>CE<sub>φ</sub>, E<sub>φ</sub>CSC, EEEE and E<sub>w</sub>E<sub>w</sub>E<sub>w</sub>E<sub>w</sub>, where the four sequential letters represent the boundary conditions for the right, top, left and bottom edges of the plate in an anticlockwise sense. As usual, ‘C’ and ‘S’ denote clamped and simple supports respectively. It should be noted that in this paper, ‘E<sub>φ</sub>’ is used to represent the edges whose transverse displacement is zero while the bending rotation is subjected to elastic rotational support with stiffness  $K_\phi(\xi)$ . Also, ‘E<sub>w</sub>’ is used to represent the edges whose rotational deformation is zero while the transverse displacement is subjected to elastic translational support with stiffness  $K_w(\xi)$ . When both translational and rotational deformation are non-zero and at least one of them is elastically constrained, the letter ‘E’ is adopted. In Table 2, all ‘E<sub>φ</sub>’, ‘E<sub>w</sub>’ and ‘E’ edges are subjected to parabolic elastic constraints with distribution  $G^a(\xi) = [1 - (\xi/L)^2]/4$ . However, ‘E<sub>φ</sub>’ means that edges with  $W(\xi) = 0, M(\xi) = K_{\phi_0}G^a(\xi)\phi(\xi)$ , ‘E<sub>w</sub>’ means that edges with  $\phi(\xi) = 0, V(\xi) = K_{w_0}G^a(\xi)W(\xi)$ , and ‘E’ means that edges have  $V(\xi) = K_{w_0}G^a(\xi)W(\xi), M(\xi) = K_{\phi_0}G^a(\xi)\phi(\xi)$  where  $K_{w_0} = D/(2a)^3$  and  $K_{\phi_0} = D/(2a)$ . The first eight dimensionless natural frequencies  $\lambda = 4\omega a^2 \sqrt{\rho h/D}$  are computed by the current SDSM when  $M = N$

and both  $M$  and  $N$  varying from 2 to 15 ( $M$  and  $N$  are respectively the number of series terms adopted for the  $x$  and  $y$  directions [28]). The computation of all results are performed on a PC equipped with a 3.40 GHz Intel 4-core processor and 8 GB of memory. The total execution time for computing the first eight natural frequencies is included in the last column of Table 2. Based on the results from Table 2, it is clearly demonstrated that the current SDSM converges very fast to exact solutions for different combinations of non-uniform and classical boundary conditions. Moreover, the SDSM exhibits an exceptionally high computational efficiency. With only 2-3 terms included in the series, the first eight natural frequencies have three to four significant digit accuracy; a ten-term series gives the natural frequencies with six significant figures literally within half a second! This is indeed an extremely high computational efficiency. It should be mentioned in passing that the first eight natural frequencies of the ‘ $E_w E_w E_w E_w$ ’ case converge even when only 2 terms are included in the series. This is expected due to the nature of the SDS formulation [27–29] which always gives exact results for fully guided plates as well as fully guided plates with translational elastic constraints irrespective of the number of terms adopted in the series.

Next, the current SDS theory is demonstrated to be robust and numerically stable for non-uniform elastic supports covering different ranges of stiffness constants. Table 3 shows the fundamental natural frequencies of an isotropic square plate with two different combinations of non-uniform elastic rotational supports and classical boundary conditions:  $CE_\phi CE_\phi$  and  $SE_\phi SE_\phi$ . In both  $CE_\phi CE_\phi$  and  $SE_\phi SE_\phi$  cases, two opposite edges ( $y = -b$  and  $y = b$ ) are ‘ $E_\phi$ ’ supported edges as defined earlier whose rotational stiffness has parabolic distribution, namely,  $W(x) = 0$  and  $M(x) = \{K_{\phi_0}[1 - (x/a)^2]/4\}\phi(\xi)$  with  $x \in [-a, a]$ . (Notice that the same parabolic distribution function is prescribed in this paper as those in the compared publications but with different expressions due to different coordinate systems adopted.) Here  $K_{\phi_0}$  is the rotational stiffness constant whose dimensionless form is defined in Table 1. The results are computed for two aspect ratios ( $a/b$ ) with the dimensionless rotational stiffness constant  $K_{\phi_0}(2a)/D$  varying from 0 to  $\infty$ . The values superscripted by ‘\*’ denotes results for plates whose ‘ $E_\phi$ ’ edges have zero rotational stiffness and therefore reduce to simply supported boundary conditions, and the results all coincide with the exact solutions for CSCS and SSSS [27] as expected. Those superscripted by ‘†’ are for edges with rotational stiffness approaching  $\infty$  to become clamped supports. These results also coincide with the exact solutions of CCCC and SCSC cases reported in [27]. The SDSM results are compared with six sets of existing solutions obtained from the Ritz method [13], Differential Quadrature method [14], Generalised Differential Quadrature method [16], Discrete Singular Convolution method [17], Ritz method based on Fourier Series [18] and the Spectral Collocation method [3] respectively. All SDSM results in Table 3 are accurate up to the last figure of the given six

Table 3: The fundamental dimensionless natural frequencies  $\lambda = 4\omega a^2 \sqrt{\rho h/D}$  for an isotropic plate ( $\nu = 0.3$ ) with two aspect ratio for two sets of BC. ‘E $_{\phi}$ ’ edges are subjected to simple supports as well as parabolic rotational elastic supports. The dimensionless rotational stiffness constant  $K_{\phi_0}(2a)/D$  varies from 0 to  $\infty$ .

BC	$a/b$	$K_{\phi_0}(2a)/D$	Ritz <sup>a</sup>	DQ <sup>b</sup>	GDQ <sup>c</sup>	DSC <sup>d</sup>	Ritz <sup>e</sup>	SC <sup>f</sup>	SDSM
CE $_{\phi}$ CE $_{\phi}$	0.5	0	23.814	23.82	23.816	23.816	23.816	23.814	<b>23.8156*</b>
		0.1	23.844	23.82	23.818	23.819	23.818	23.844	<b>23.8180</b>
		1	23.876	23.85	23.839	23.843	23.839	23.876	<b>23.8385</b>
		10	24.136	24.01	23.996	24.019	23.996	24.136	<b>23.9964</b>
		100	24.561	24.41	24.393	24.410	24.393	–	<b>24.3932</b>
		$\infty$	24.566	24.60	24.578	24.579	24.578	24.650	<b>24.5777<sup>†</sup></b>
	1	0	28.951	28.96	28.951	28.952	28.951	28.951	<b>28.9509*</b>
		0.1	28.969	28.98	28.966	28.970	28.966	28.966	<b>28.9663</b>
		1	28.219	29.12	29.102	29.128	29.103	29.103	<b>29.1026</b>
		10	32.179	30.24	30.222	30.383	30.222	30.222	<b>30.2223</b>
		100	35.379	33.82	33.796	33.960	33.795	–	<b>33.7955</b>
		$\infty$	35.992	36.01	35.985	35.987	35.985	35.992	<b>35.9852<sup>†</sup></b>
SE $_{\phi}$ SE $_{\phi}$	0.5	0	Anal. <sup>a</sup>	DQ <sup>b</sup>	GDQ <sup>c</sup>	DSC <sup>d</sup>	Ritz <sup>e</sup>	SC <sup>f</sup>	SDSM
		0.1	12.337*	12.34	12.337	12.337	12.349	12.337	<b>12.3370*</b>
		1	12.341	12.34	12.341	12.340	12.354	12.341	<b>12.3413</b>
		10	12.372	12.38	12.379	12.362	12.391	12.379	<b>12.3791</b>
		100	12.621	12.66	12.666	12.550	12.674	12.666	<b>12.6657</b>
		$\infty$	13.319	13.37	13.364	13.207	13.366	–	<b>13.3640</b>
	1	0	13.688	13.70	13.686	13.686	13.686	13.686	<b>13.6858<sup>†</sup></b>
		0.1	19.739*	19.74	19.734	19.739	19.748	19.739	<b>19.7392*</b>
		1	19.757	19.76	19.761	19.764	19.770	19.761	<b>19.7609</b>
		10	19.915	19.95	19.951	19.985	19.960	19.951	<b>19.9513</b>
		100	21.235	21.49	21.487	21.701	21.493	21.487	<b>21.4867</b>
		$\infty$	25.799	26.13	26.147	26.356	26.149	–	<b>26.1474</b>
		$\infty$	28.951	28.98	28.951	28.951	28.950	28.951	<b>28.9509<sup>†</sup></b>

<sup>a</sup> Ritz or Analytical [13];

<sup>b</sup> Differential Quadrature [14];

<sup>c</sup> Generalised Differential Quadrature [16];

<sup>d</sup> Discrete Singular Convolution [17];

<sup>e</sup> Ritz (Fourier) [18];

<sup>f</sup> Spectral Collocation [3];

significant figures, which have without doubt the highest accuracy compared to the other methods. The results computed from both the Generalised Differential Quadrature method [16] and the Spectral Collocation method [3] all agree with the SDSM results for the first five significant figures, and therefore they are the most accurate results other than the SDSM results.

Now the current SDS theory is used to revisit the case of a square isotropic plate with different combinations of classical BC and parabolic rotational constraints. Some of the results for these cases are available in the literature [17, 18]. All SDSM results are presented with six significant figures which serve as benchmark solutions. Side by side, the results by using the Fourier series based analytical method (FSA) [18] as well as the Discrete Singular Convolution method (DSC) [17] are given, both of which have accuracy with only three to four significant figures.

In order to illustrate the applicability of the method to arbitrary non-uniform elastic supports, the current SDS theory is also used to revisit a complex case that

Table 4: The first eight dimensionless natural frequencies of six cases for a square isotropic plate ( $2a \times 2b = 2L \times 2L$  and  $\nu = 0.3$ ) with different combinations of classical BC and parabolic rotational constraints (denoted by ‘E $_{\phi}$ ’ with  $K_{\phi}(\xi) = D/(2a)[1 - (\xi/L)^2]/4$ ). Comparisons are made among the current SDSM, the Fourier series based analytical method (FSA) [18] and the Discrete Singular Convolution method (DSC) [17].

BC	Method	$\lambda = 4\omega a^2 \sqrt{\rho h/D}$							
		1	2	3	4	5	6	7	8
E $_{\phi}$ SSC	<b>SDSM</b>	<b>23.7356</b>	<b>51.8395</b>	<b>58.6776</b>	<b>86.2191</b>	<b>100.462</b>	<b>113.243</b>	<b>133.913</b>	<b>140.895</b>
	FSA	23.749	51.862	58.695	86.27	100.485	113.262	133.98	140.96
	DSC	23.75	51.868	58.685	86.237	100.498	113.254	133.942	140.915
E $_{\phi}$ SCS	<b>SDSM</b>	<b>23.7807</b>	<b>51.7196</b>	<b>58.8278</b>	<b>86.2346</b>	<b>100.291</b>	<b>113.426</b>	<b>133.851</b>	<b>140.976</b>
	FSA	23.794	51.742	58.845	86.285	100.313	113.445	133.918	141.041
	DSC	23.803	51.728	58.861	86.256	100.296	113.469	133.868	141.012
E $_{\phi}$ CCS	<b>SDSM</b>	<b>27.1721</b>	<b>60.6381</b>	<b>60.9043</b>	<b>92.9329</b>	<b>114.627</b>	<b>114.849</b>	<b>145.877</b>	<b>146.172</b>
	FSA	27.181	60.639	60.926	92.96	114.631	114.868	145.877	146.243
	DSC	27.192	60.654	60.931	92.957	114.643	114.89	145.912	146.207
E $_{\phi}$ CSC	<b>SDSM</b>	<b>29.0264</b>	<b>54.9032</b>	<b>69.3545</b>	<b>94.6655</b>	<b>102.409</b>	<b>129.109</b>	<b>140.325</b>	<b>154.822</b>
	FSA	29.026	54.903	69.354	94.665	102.408	129.108	140.324	154.82
	DSC	29.039	54.932	69.365	94.689	102.447	129.131	140.363	154.858
CE $_{\phi}$ E $_{\phi}$ S	<b>SDSM</b>	<b>23.8697</b>	<b>51.8848</b>	<b>58.859</b>	<b>86.3192</b>	<b>100.483</b>	<b>113.441</b>	<b>133.973</b>	<b>141.026</b>
	FSA	23.883	51.907	58.877	86.369	100.506	113.46	134.04	141.091
	DSC	23.906	51.921	58.897	86.355	100.523	113.488	134.013	141.07
SE $_{\phi}$ CE $_{\phi}$	<b>SDSM</b>	<b>23.8256</b>	<b>52.0048</b>	<b>58.709</b>	<b>86.3039</b>	<b>100.655</b>	<b>113.259</b>	<b>134.035</b>	<b>140.945</b>
	FSA	23.839	52.027	58.727	86.354	100.678	113.278	134.102	141.01
	DSC	23.855	52.061	58.721	86.337	100.725	113.272	134.087	140.974

is reported in [18]. It is an isotropic rectangular plate with four edges subjected to completely different non-uniform elastic supports characterized as follows.

$$K_{w1}(y) = [5/4 + y/(2b) + y^2/(2b)^2]D/(2a)^3, \quad K_{\phi1}(y) = D/(2a), \quad x = a, \quad (22a)$$

$$K_{w2}(x) = D/(2a)^3, \quad K_{\phi2}(x) = D/(2a), \quad y = b, \quad (22b)$$

$$K_{w3}(y) = [3/2 + y/(2b)]D/(2a)^3, \quad K_{\phi3}(y) = [3/2 + y/(2b)]D/(2a), \quad x = -a, \quad (22c)$$

$$K_{w4}(x) = [1 - \sin(\pi x/(2a))]D/(2a)^3, \quad K_{\phi4}(x) = [1 - \sin(\pi x/(2a))]D/(2a), \quad y = -b. \quad (22d)$$

Again, the above expressions for the same stiffness functions are different from those given in [18] due to different coordinate systems adopted. In this paper,  $x \in [-a, a], y \in [-b, b]$  whereas in [18],  $x \in [0, a], y \in [0, b]$ . It should be mentioned in passing that problems of this nature can not be easily treated by some other methods such as the DSC method [17], because the DSC method appears to be only capable of handling non-uniform elastic rotational supports (‘E $_{\phi}$ ’) but it becomes inadequate to treat non-uniform translational elastic supports (‘E $_w$ ’ or ‘E’). In the SDSM implementation, one element is used with only 20 terms in the series, which gives ten natural frequencies within 1.5 s, and all SDSM results have six significant figures as shown in Table 5. The results are compared with those computed by the Ritz method using the Fourier series (Ritz (Fourier)) [18] as well as the finite element method (FEM) using a  $100 \times 100$  mesh. It can be seen that the results by the Ritz (Fourier) and the FEM have only two to three significant digit precision. The inaccuracy of the Ritz (Fourier) method [18] might be due to

Table 5: Dimensionless natural frequency parameter  $\lambda = 4\omega a^2 \sqrt{\rho h/D}$  for isotropic rectangular plates ( $\nu = 0.3$ ) with three different aspect ratio, which are subjected to a complex combination of different non-uniform elastic supports along the four edges as prescribed in Eq. (22).

$a/b$		1	2	3	4	5	6	7	8	9	10
1	SDSM	<b>2.17536</b>	<b>5.19700</b>	<b>5.69328</b>	<b>14.9857</b>	<b>24.2020</b>	<b>27.1478</b>	<b>37.0910</b>	<b>37.4995</b>	<b>64.6553</b>	<b>65.4538</b>
	Ritz (Fourier) <sup>a</sup>	2.17	5.14	5.71	15.00	24.17	27.14	37.17	37.53	64.56	65.48
	FEM <sup>b</sup>	2.18	5.09	5.78	14.98	24.17	27.16	37.12	37.50	64.57	65.49
2	SDSM	<b>2.59353</b>	<b>5.84346</b>	<b>13.4285</b>	<b>25.7436</b>	<b>29.8778</b>	<b>60.6889</b>	<b>64.5266</b>	<b>95.1368</b>	<b>104.249</b>	<b>109.990</b>
	Ritz (Fourier) <sup>a</sup>	2.58	5.84	13.24	25.75	29.82	60.68	64.53	94.94	104.3	110.1
4	SDSM	<b>3.25733</b>	<b>6.17952</b>	<b>25.6793</b>	<b>37.6219</b>	<b>64.1624</b>	<b>64.9265</b>	<b>114.628</b>	<b>122.125</b>	<b>175.881</b>	<b>199.558</b>
	Ritz (Fourier) <sup>a</sup>	3.23	6.18	25.68	36.85	64.16	64.96	114.7	122.1	175.9	199.6

<sup>a</sup> Ritz method based on Fourier series [18]; <sup>b</sup> Finite element method with  $100 \times 100$  elements [18].

the numerical instability encountered in the computation when using the method.

Next, another problem is investigated by the current SDSM to consider plates with elastic coupling constraints. It is a system of two isotropic rectangular plates (denoted by plates 1 and 2) elastically coupled by a uniform elastic coupling constraint. The material properties for both plates are: Young's modulus  $E = 2.16 \times 10^{11} N/m^2$ , Poisson's ratio  $\nu = 0.28$  and density  $\rho = 7800 kg/m^3$ . The two plates have thickness  $h_1 = h_2 = 0.008 m$  length  $2a_1 = 1.4 m$ ,  $2a_2 = 1.0 m$  and width  $2b_1 = 2b_2 = 1.2 m$ . They are horizontally connected along the edges of length  $1.2 m$  that are parallel to the  $y$  axis. All of the plates edges are simply supported except for the two elastically coupled edges. Both of the translational and rotational coupling stiffnesses are uniformly distributed with the coupling stiffness constants  $C_w$  and  $C_\phi$  taking different values for two cases: (i)  $C_w = C_\phi = 10^5$  and (ii)  $C_w = C_\phi = 10^{15}$  to model the rigid connection situation  $C_w = C_\phi = \infty$ . In the SDSM implementation, two elements are used for this case. The SDS matrix for the elastic coupling constraints is formulated following the procedure described in Section 2.2.2, which is superposed directly onto that of the two-plate system. All SDSM results are presented with five significant figures. For the first case where  $C_w = C_\phi = 10^5$ , two sets of the SDSM results are computed, one considering rotatory inertia in the plate theory (superscripted by '1') and the other without (superscripted by '0'). It is clear that the SDSM results considering the rotatory inertia agree very well with the FEM solutions. The relative errors are within 0.01%. The results without considering the rotatory inertia are also computed by using the SDSM, which are compared with the Ritz (Fourier) solutions [26]. The second half of Table 6 shows the same model as the previous one but with rigid connections  $C_w = C_\phi = \infty$  on the coupled edges. This case is essentially equivalent to a Navier plate for which closed-form exact solution exists. It can be seen that all SDSM results coincide with the exact Navier solution whereas the Ritz (Fourier) solution [26] for both cases only have two to three digit accuracy. Apparently, the current method gives much more accurate results than other methods and therefore will serve as benchmarks.

Table 6: Natural frequencies (all results in Hz) for two elastically coupled plates with two sets of uniform translational  $C_w$  and rotational  $C_\phi$  coupling stiffness. The first set is with  $C_w = C_\phi = 10^5$  whereas the second set for  $C_w = C_\phi = 10^{15}$  to model rigid connection situation  $C_w = C_\phi = \infty$ .

Mode	1	2	3	4	5	6	7	8	9	10
$C_w = C_\phi = 10^5$										
SDSM <sup>1</sup>	<b>16.965</b>	<b>21.228</b>	<b>36.012</b>	<b>54.290</b>	<b>57.919</b>	<b>60.432</b>	<b>72.838</b>	<b>77.250</b>	<b>97.035</b>	<b>115.54</b>
FEM [18] <sup>1</sup>	16.965	21.228	36.011	54.290	57.922	60.438	72.836	77.250	97.034	115.52
SDSM <sup>0</sup>	<b>16.965</b>	<b>21.228</b>	<b>36.013</b>	<b>54.295</b>	<b>57.924</b>	<b>60.437</b>	<b>72.846</b>	<b>77.258</b>	<b>97.048</b>	<b>115.55</b>
Ritz (Fourier) [18] <sup>0</sup>	16.996	21.275	36.131	54.470	57.956	60.498	73.021	77.475	97.395	115.95
SDSM <sup>1</sup> /FEM <sup>1</sup> (%)	0.00	0.00	0.00	0.00	0.00	0.01	0.00	0.00	0.00	-0.01
SDSM <sup>0</sup> /Ritz <sup>0</sup> (%)	0.18	0.22	0.33	0.32	0.06	0.10	0.24	0.28	0.36	0.34
$C_w = C_\phi = \infty$										
SDSM <sup>0</sup>	<b>17.261</b>	<b>27.618</b>	<b>44.880</b>	<b>58.689</b>	<b>69.045</b>	<b>69.045</b>	<b>86.307</b>	<b>100.12</b>	<b>110.47</b>	<b>127.73</b>
Navier (Exact) <sup>0</sup>	17.261	27.618	44.880	58.689	69.045	69.045	86.307	100.12	110.47	127.73
Ritz (Fourier) [18] <sup>0</sup>	17.299	27.745	45.016	58.725	69.163	69.207	86.545	100.17	110.77	127.78
SDSM <sup>0</sup> /Navier <sup>0</sup> (%)	0.00	0.00	0.00	0.00	0.00	0.00	0.00	0.00	0.00	0.00
SDSM <sup>0</sup> /Ritz <sup>0</sup> (%)	0.22	0.46	0.30	0.06	0.17	0.24	0.24	0.05	0.27	0.04

<sup>1</sup> consider rotatory inertia in plate elements (for SDSM: classical plate theory +  $I_2$ ); <sup>0</sup> no rotatory inertia in plate elements (classical plate theory only).

### 3.2. A hinged composite plate with a uniform or non-uniform elastic support and a mass attachment

A hinged plate problem is of common practical significance which is a model for hinged gates in the field of civil, aeronautical and hydraulic engineering. More than often, those gates are subjected to uniform or non-uniform rotational supports along the hinged edges ( $K_\phi(\xi)$ ) to control and monitor the gate. Also, uniformly or non-uniformly distributed mass attachments ( $m(\xi)$ ) can also be attached to the edge opposite to the hinged edge, see Fig. 2. The SDS development in this research allows modelling such problems accurately and efficiently.

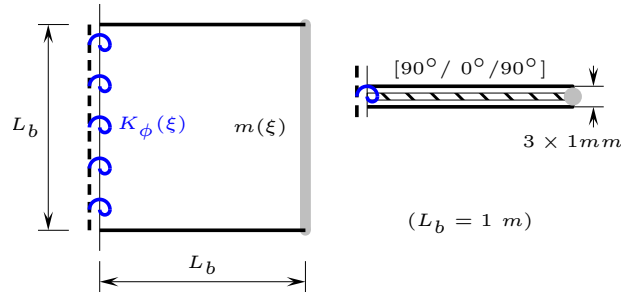


Figure 2: A symmetric cross-ply laminated plate subject to a uniformly or non-uniform rotational elastic support ( $K_\phi(\xi)$ ) on the hinged edge, and uniform or non-uniform line-mass attachment on the other edge ( $m(\xi)$ ).

In Fig. 2, the laminated plate is made of T-graphite/epoxy material for which  $E_1 = 185 \text{ GPa}$ ,  $E_2 = 10.5 \text{ GPa}$ ,  $G_{12} = 7.3 \text{ GPa}$ ,  $\nu_{12} = 0.28$ ,  $\rho = 1600 \text{ kg/m}^3$ . The plate has the dimension  $1 \text{ m} \times 1 \text{ m}$  consisting of three laminae with the stacking sequence  $[90^\circ/0^\circ/90^\circ]$ . Each ply is  $1 \text{ mm}$  thick. The left-hand edge is hinged and also subjected to uniform or non-uniform rotational elastic supports with stiffness distribution  $K_\phi(\xi)$ . Along the right-hand edge, uniformly or non-uniformly

Table 7: The first 10 natural frequencies of a hinged cross-ply laminated ( $[90^\circ/0^\circ/90^\circ]$ ) plate subjected to uniform or non-uniform rotational elastic support as well as line mass attachments as indicated in Fig. 2. (For all results, rotatory inertia is considered in the Kirchhoff plate theory.)

	Natural frequencies (Hz)									
	1	2	3	4	5	6	7	8	9	10
Case 1	<b>0.90318</b>	<b>2.5916</b>	<b>7.5659</b>	<b>10.870</b>	<b>15.918</b>	<b>23.149</b>	<b>26.807</b>	<b>33.861</b>	<b>36.360</b>	<b>47.486</b>
Case 2	<b>0.89976</b>	<b>2.5774</b>	<b>7.5304</b>	<b>10.777</b>	<b>15.918</b>	<b>23.034</b>	<b>26.545</b>	<b>33.854</b>	<b>36.306</b>	<b>47.216</b>
Case 3	<b>0.89454</b>	<b>2.8077</b>	<b>7.6647</b>	<b>11.004</b>	<b>17.583</b>	<b>23.433</b>	<b>27.361</b>	<b>35.836</b>	<b>37.582</b>	<b>47.759</b>
Case 4	<b>0.89115</b>	<b>2.7917</b>	<b>7.6277</b>	<b>10.917</b>	<b>17.566</b>	<b>23.311</b>	<b>27.121</b>	<b>35.791</b>	<b>37.542</b>	<b>47.406</b>

distributed mass  $m(\xi)$  with no rotatory inertia is attached. The rest two edges are free, see Fig. 2. (Therefore, in this model,  $\xi$  represents  $y$  only.) The following four cases with different distribution of  $K_\phi(\xi)$  and  $m(\xi)$  are considered in the analysis

$$\text{Case 1: } K_\phi(\xi) = K_{\phi_0}, \quad m(\xi) = m_0, \quad (23a)$$

$$\text{Case 2: } K_\phi(\xi) = K_{\phi_0}[1 - (\xi/L)^2], \quad m(\xi) = m_0, \quad (23b)$$

$$\text{Case 3: } K_\phi(\xi) = K_{\phi_0}, \quad m(\xi) = m_0(1 + \xi/L), \quad (23c)$$

$$\text{Case 4: } K_\phi(\xi) = K_{\phi_0}[1 - (\xi/L)^2], \quad m(\xi) = m_0(1 + \xi/L). \quad (23d)$$

Here,  $\xi \in [-L, L]$  ( $L = L_b/2 = 0.5 m$ ) and the dimensionless rotational stiffness takes the value  $K_{\phi_0}L_b/D_x = 500$  ( $D_x$  is the bending stiffness of the laminated plate in the  $x$  direction) and the dimensionless mass constant  $m_0L_b/m_p = 0.5$  ( $m_p$  is the total mass of the plate).

In the SDSM implementation, only one SDS element is used with 20 terms included in the series, and a linear combination of  $\mathbf{G}^a$  matrices for the dimensionless distribution functions  $1, \xi/L$  and  $(\xi/L)^2$  as given in Appendix A are used for the corresponding distributions of  $K_\phi(\xi)$  and  $m(\xi)$ . The first 10 natural frequencies for these three cases are computed and tabulated in Table 7. All results have accuracy of five significant figures, and the total computation time for computing the ten natural frequencies is less than 1.5 s. The 1st, 2nd and 4th mode shapes of Cases 2 and 4 are given in Fig. 3. Some important observations based on the results shown in Table 7 and Fig. 3 can be made: (i) All natural frequencies for Case 2 (or 4) are smaller than those for Case 1 (or 3) as expected, since Case 2 (or 4) has smaller rotational stiffness distribution than that of Case 1 (or 3). (ii) Even though the rotational stiffness  $K_\phi(\xi)$  as well as the total mass of the attachment ( $\int_{-L}^L m(\xi)d\xi = m_0L_b = 2m_0L$ ) of Cases 1 and 3 (also Cases 2 and 4) are the same, the mass attachment with linearly non-uniform distribution decreases the fundamental natural frequency and yet increases all other natural frequencies, i.e., the 2nd-10th modes. Also, the difference between the mode shapes of Cases 1 and 3 (or between Cases 2 and 4) is significant, for example, see Fig. 3 for the comparison between the mode shapes of Cases 2 and 4. This is expected because, compared to a uniformly distributed line mass, a linearly non-uniform mass makes

the deformation become unsymmetrical therefore exerts more coupling effects on the plate vibration which increases the natural frequencies corresponding to coupling mode shapes (2nd-10th modes). This finding is highly significant for the design of structures to improve their dynamic behaviour by modifying the mass distribution.

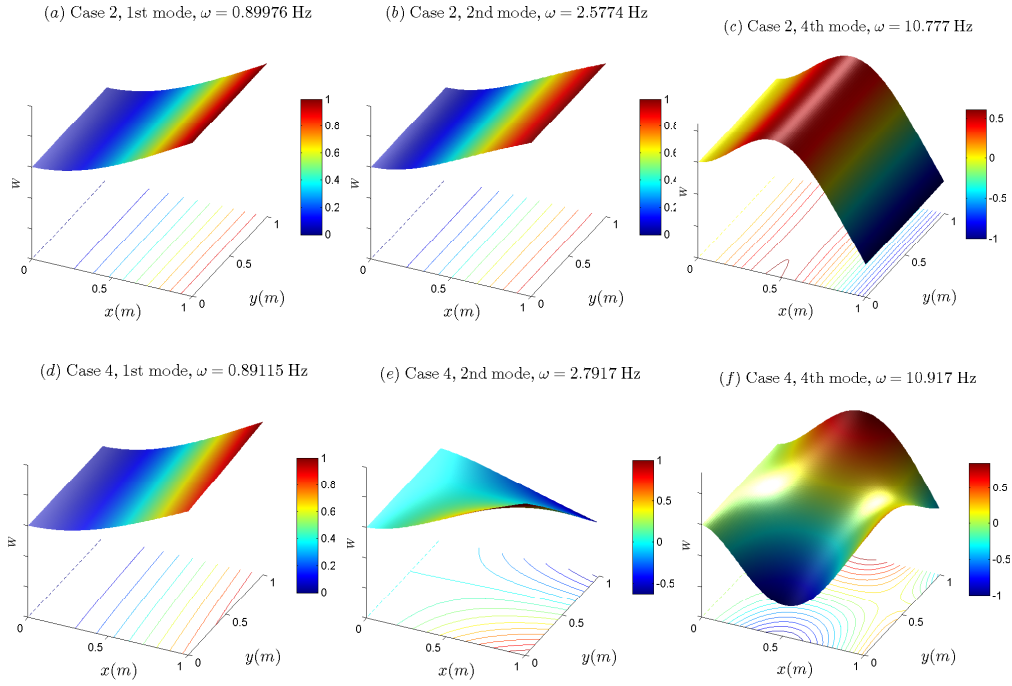


Figure 3: The 1st, 2nd, 4th natural modes of a hinged composite plate as shown in Fig. 2 for two cases: (a) – (c) are for Case 2 (given in Eq. (23b)) with uniform mass attachments whereas (d) – (f) are for Case 4 (given in Eq. (23d)) with linearly non-uniform mass attachments.

### 3.3. Uniformly or non-uniformly elastically coupled composite plate systems with attached masses

In this section, the SDSM is applied to an elastically coupled composite plate system consisting of two laminated plates, see Fig. 4. This model has wide applications in engineering such as an optical beam pointing system in areas like laser communications and aerospace applications [23]. This problem also frequently emerges in suspension systems in areas of automotive and precision machinery. In Fig. 4, the upper plate (denoted as ‘Plate I’) is elastically coupled to the lower plate (‘Plate II’). Here, Plate I normally serves as a platform equipped with vibration sensitive devices, and Plate II models the parent structure. The elastic coupling constraints are used to reduce the structural vibration transmitted from

the parent structure (Plate II) to the platform (Plate I). The current research provides an efficient and convenient approach to investigate the coupling effects so as to pave the way for further optimisation studies of such structures to reduce vibration.

In this example, Plate I is made of a square T-graphite epoxy lamina with ply angle  $0^\circ$ , thickness  $1\text{ mm}$  and dimension  $L_b \times L_b = 1\text{ m} \times 1\text{ m}$ . There are uniformly or non-uniformly distributed mass  $m(\xi)$  (no rotatory inertia is taken into account for the mass attachments) around the four edges of Plate I. Plate II is composed of three T-graphite epoxy laminae with the stacking sequence  $[90^\circ/0^\circ/90^\circ]$  ( $3 \times 1\text{ mm}$ ) and dimension  $3L_b \times L_b = 3\text{ m} \times 1\text{ m}$ , see Fig. 4. (Here, both plates are chosen to have simple geometries just for illustrative purposes. Of course, the present theory can handle more complex and general cases.) The material properties is:  $E_1 = 185\text{ GPa}$ ,  $E_2 = 10.5\text{ GPa}$ ,  $G_{12} = 7.3\text{ GPa}$ ,  $\nu_{12} = 0.28$ ,  $\rho = 1600\text{ kg/m}^3$ . Plate I and Plate II are elastically coupled by uniform or non-uniform translational coupling constraints  $C_w(\xi)$  along four line nodes of both plates (indicated by red dashed lines in Fig. 4). Plate II is clamped on the left and right edges whereas the other edges are free, see Fig. 4. The following four cases are discussed for this problem with different distribution of translational elastic coupling constraints  $C_w(\xi)$  and mass attachments  $m(\xi)$ .

$$\begin{aligned}
\text{Case 1:} \quad & C_w(\xi) = C_{w0}, & m(\xi) &= m_0, \\
\text{Case 2:} \quad & C_w(\xi) = C_{w0}[1 + (\xi/L)^2], & m(\xi) &= m_0, \\
\text{Case 3:} \quad & C_w(\xi) = C_{w0}, & m(\xi) &= m_0[1 - (\xi/L)^2], \\
\text{Case 4:} \quad & C_w(\xi) = C_{w0}[1 + (\xi/L)^2], & m(\xi) &= m_0[1 - (\xi/L)^2],
\end{aligned}$$

where  $\xi$  represents either  $x$  or  $y$  with  $\xi \in [-L, L]$  ( $L = L_b/2 = 0.5\text{ m}$ ); the dimensionless translational coupling stiffness constant takes  $C_{w0}L_b^3/D_{xI} = 200$  ( $D_{xI}$  is the bending stiffness of Plate I in the  $x$ -direction); the dimensionless mass constant is  $m_0L_b/m_I = 0.5$  ( $m_I$  is the total mass of Plate I). It should be borne in mind that the coupling constraints  $C_{w0}[1 + (\xi/L)^2]$  are ‘stiffer’ than  $C_{w0}$ , whereas the mass attachments  $m_0[1 - (\xi/L)^2]$  are ‘lighter’ than  $m_0$ .

Table 8: The first 10 natural frequencies of an elastically coupled composite plate system with mass attachments as shown in Fig. 4. (Rotatory inertia is considered in the plate theory.)

	Natural frequencies (Hz)									
	1	2	3	4	5	6	7	8	9	10
Case 1	<b>0.89686</b>	<b>1.7889</b>	<b>2.5854</b>	<b>4.3316</b>	<b>5.3237</b>	<b>5.8319</b>	<b>7.6803</b>	<b>8.0190</b>	<b>8.8364</b>	<b>10.849</b>
Case 2	<b>0.89236</b>	<b>1.7737</b>	<b>2.5565</b>	<b>4.1387</b>	<b>5.2290</b>	<b>5.8231</b>	<b>7.3318</b>	<b>7.5920</b>	<b>7.8896</b>	<b>8.2326</b>
Case 3	<b>0.86277</b>	<b>1.6663</b>	<b>2.4605</b>	<b>3.9210</b>	<b>5.2955</b>	<b>5.7776</b>	<b>7.5048</b>	<b>7.8632</b>	<b>8.4774</b>	<b>10.351</b>
Case 4	<b>0.85702</b>	<b>1.6431</b>	<b>2.4091</b>	<b>3.6116</b>	<b>5.1220</b>	<b>5.7277</b>	<b>6.3333</b>	<b>6.4774</b>	<b>6.6417</b>	<b>7.5998</b>

In the SDSM implementation, Plate I and Plate II are modelled by using one and three SDS elements respectively with 20 terms included in the series. The SDS matrices of the mass attachments  $m(\xi)$  are directly superposed to the sub-SDS matrices corresponding to the four line DOF of Plate I. The SDS matrices

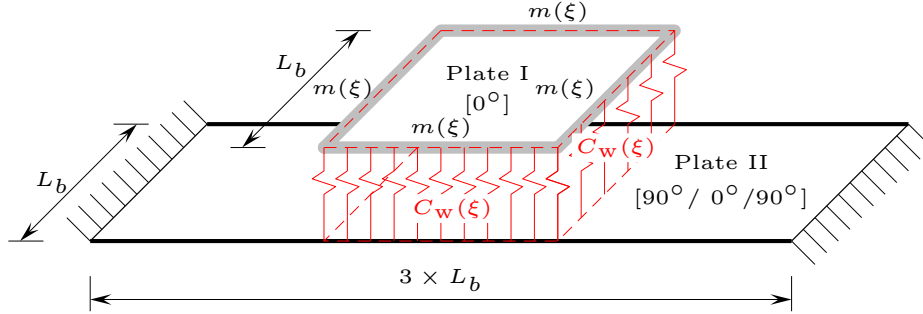


Figure 4: A square lamina  $[0^\circ]$  (denoted by ‘Plate I’) with line mass attachments  $m(\xi)$  along all its edges, is elastically coupled (with translational coupling stiffness  $C_w(\xi)$ ) to a laminated parent structure (denoted by ‘Plate II’, with stacking sequence  $[90^\circ/0^\circ/90^\circ]$ ). Length:  $L_b = 1 m$ .

of the translational elastic coupling constraints  $C_w(\xi)$  are directly superposed to the corresponding sub-SDS matrices for the four pairs of the coupled line DOF of Plates I and II. The first 10 natural frequencies are computed for the four cases all with five significant figures, see Table 8. Some representative mode shapes for Case 1 (with uniform coupling constraints and uniform mass attachments) are shown in Fig. 5. It is clear that the 2nd and the 3rd natural modes are dominated by the parent structure (Plate II) whereas the 5th and 20th modes are Plate I dominated. One of the useful conclusions drawn from this problem is: stiffer coupling constraints (Cases 2 verse 1; Cases 4 verse 3) and lighter attached mass (Cases 3 verse 1; Cases 4 verse 2) for such a problem decrease the natural frequencies. This is expected since the coupling constraints introduce more interacting modes whereas mass attachments generally ‘impede’ the structural motion.

### 3.4. A composite aircraft wing elastically coupled with flap and attached with store, missile and engine (non-uniform mass)

The modal analysis of aircraft wings is a mandatory consideration in aircraft design particularly from an aeroelastic point of view [39, 40], as it provides the fundamental information to aid aerodynamic analysis [41, 42]. The presence of stores, engines as well as flap affects the dynamic properties of the aircraft significantly and therefore, influences the aeroelastic stability as well as the maneuverability of the aircraft in operation. The Goland wing [43] is a cantilevered rectangular wing model which has received wide attention from an aeroelastic analysis perspective, e.g, see [39, 40]. The majority of the existing work on modal analysis simply use a one-dimensional beam model such as in [41]. More detailed analysis considered it as a cantilevered plate using commercial software [39, 40]. In the plate model, it appears that only uniformly distributed mass has been used for the

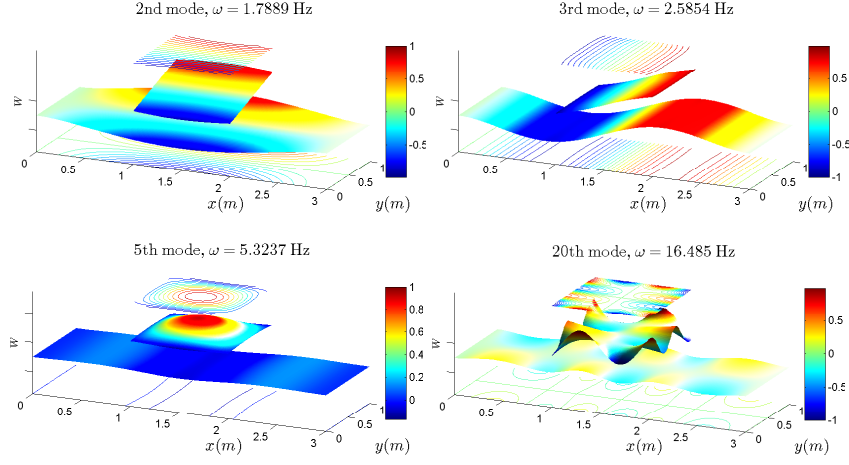


Figure 5: The 2nd, 3rd, 5th and 20th natural modes of an elastically coupled composite plate system with mass attachments (corresponding to Case 1 in Table 8). The two (upper and lower) contours shown in each mode shape plots are for Plate I and Plate II respectively.

store. The present research proposes a novel analytical method for modal analysis of composite rectangular wing with uniform or non-uniform attachments like engine as well as elastically coupled flap in an efficient and elegant way.

The composite wing to be analysed using the current SDSM has the same dimensions as the Goland wing reported in the literature [39, 40]. However, this wing model is made of carbon fibre/epoxy material:  $E_1 = 161.0 \text{ GPa}$ ,  $E_2 = 11.38 \text{ GPa}$ ,  $G_{12} = 5.170 \text{ GPa}$ ,  $\nu_{12} = 0.38$ ,  $\rho = 1560 \text{ kg/m}^3$ . Moreover, it is elastically coupled with a flap as well as attached with a store, a missile and an engine with non-uniform mass and inertia distribution, see Fig. 6. The characteristic data are included in Table 9. The data reflect a proper scale model for a real aircraft wing.

Twelve different cases with or without the store, missile, engine attachments

Table 9: Characteristic data of the flap wing with attachments as shown in Fig. 6. In this table,  $\xi \in [-L, L]$  and  $L = H_{wg}/2$ .

Wing	Dimension: $L_{wg} \times H_{wg} = 6.096 \text{ m} \times 1.829 \text{ m}$ ; Stacking sequence: 3 plies carbon fibre/epoxy laminae $[0^\circ/90^\circ/0^\circ]$ ( $3 \times 2.032 \text{ cm}$ ).
Flap	Dimension: $L_{fp} \times H_{fp} = 6.096 \text{ m} \times 0.6096 \text{ m}$ ; Stacking sequence: 1 ply $[0^\circ]$ carbon fibre/epoxy lamina ( $1 \times 3.048 \text{ cm}$ ); Elastically coupled to the wing with uniform rotational coupling constraint with stiffness $K_\phi \equiv 10^5 \text{ kgm}$ .
Store	Mass: $m_{st}(\xi) = 180 \text{ kg/m}$ ; Rotatory inertia: $I_{2st}(\xi) = 0.75 \text{ kgm}$ ; Location: Wing tip.
Missile	Mass: $m_{ms}(\xi) = 180 \text{ kg/m}$ ; Rotatory inertia: $I_{2ms}(\xi) = 30 \text{ kgm}$ ; Location: $d_{ms} = 4/5 L_{wg}$ from the wing root.
Engine	Mass: $m_{eg}(\xi) = 75(1 + \xi/L)(5 - \xi/L) \text{ kg/m}$ ; Rotatory inertia: $I_{2eg}(\xi) = 80(1 + \xi/L)^2 \text{ kgm}$ ; Location: $d_{eg} = 1/5 L_{wg}$ from the wing root.

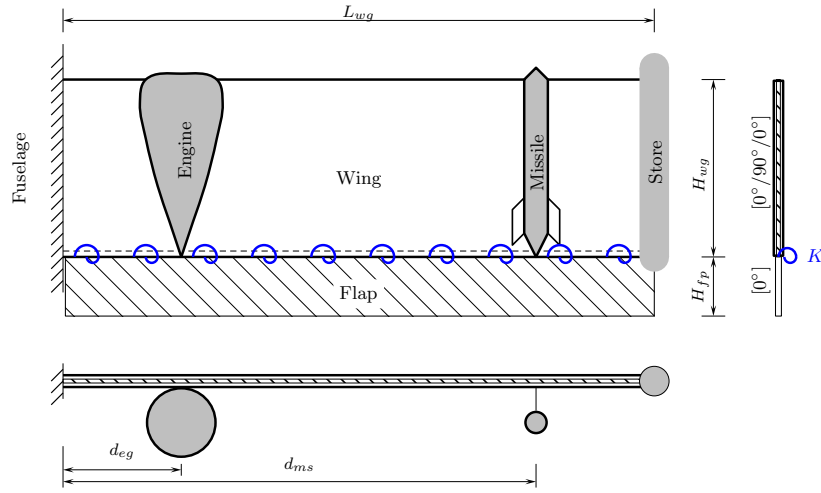


Figure 6: A composite Goland wing with rotationally coupled flap as well as engine, missile and store attachments. The characteristics of all components are given in Table 9.

and elastically coupled flap are considered in the analysis by using the current SDSM. It should be kept in mind that the engine has almost double the total mass as that of the store and missile. The engine, missile and store are amounted at  $1/5$  span from the wing root,  $4/5$  span from the wing root and at the wing tip, respectively. The first 10 natural frequencies are shown in Table 10, all with four significant figures. Different number of SDS elements are used in these 12 cases (the values are given in the parentheses of the first column of Table 10) to facilitates ‘attaching’ the mass attachments and coupling constraint by the corresponding line nodes. Of course, the cases using more SDS elements can handle all of the cases using less elements. The first six natural mode shapes of the last case in Table 10 (Wg+Fp+Eg+St+Ms) for the wing attached with an engine, a store, a missile as well as elastically coupled with a flap are shown in Fig. 7. Some interesting findings can be carefully observed from the analysis which can be listed as follows.

- (i) Any additional mass attachments or flap coupling decrease all of the natural frequencies, as expected.
- (ii) The elastically coupled flap and the engine mass attached near the wing root play a more significant role in reducing the natural frequencies than the store and missile. Additionally, the presence of both the flap and engine results in more reduction in the higher natural frequencies than in the lower ones. This is because the presence of both the flap and the non-uniform engine mass introduces significant coupling effects. The coupling effects arising from the flap is obvious, for example, see Figs. 7(d), (e) and (f). For the engine, it is also perfectly understandable, because the engine has larger

Table 10: The first 10 natural frequencies (in Hz) of the composite wing as shown in Fig. 6 for 12 different cases. Wg, Fp, Eg, St and Ms in the first column represent the presence of the wing, flap, engine, store and missile, respectively. The values in the parentheses in the first column indicate the number of SDS elements used in the modelling.

Case	1	2	3	4	5	6	7	8	9	10
Wg (1)	<b>2.654</b>	<b>6.587</b>	<b>16.62</b>	<b>24.10</b>	<b>46.51</b>	<b>54.04</b>	<b>62.96</b>	<b>72.84</b>	<b>91.23</b>	<b>96.05</b>
Wg+St (1)	<b>1.764</b>	<b>4.690</b>	<b>13.21</b>	<b>18.47</b>	<b>34.24</b>	<b>39.58</b>	<b>45.14</b>	<b>67.09</b>	<b>73.44</b>	<b>80.36</b>
Wg+Ms (2)	<b>2.057</b>	<b>5.141</b>	<b>15.81</b>	<b>22.75</b>	<b>41.07</b>	<b>47.27</b>	<b>47.74</b>	<b>68.59</b>	<b>80.00</b>	<b>83.75</b>
Wg+Eg (2)	<b>2.631</b>	<b>6.438</b>	<b>13.91</b>	<b>20.11</b>	<b>33.42</b>	<b>39.75</b>	<b>42.60</b>	<b>51.92</b>	<b>57.43</b>	<b>63.73</b>
Wg+Fp (2)	<b>2.471</b>	<b>5.066</b>	<b>14.15</b>	<b>18.44</b>	<b>23.33</b>	<b>25.12</b>	<b>33.62</b>	<b>36.18</b>	<b>47.38</b>	<b>56.57</b>
Wg+St+Ms (2)	<b>1.552</b>	<b>4.083</b>	<b>12.31</b>	<b>17.51</b>	<b>32.63</b>	<b>33.74</b>	<b>38.06</b>	<b>54.48</b>	<b>69.02</b>	<b>72.27</b>
Wg+Eg+St (2)	<b>1.758</b>	<b>4.649</b>	<b>11.63</b>	<b>16.27</b>	<b>27.99</b>	<b>34.24</b>	<b>34.83</b>	<b>42.10</b>	<b>49.69</b>	<b>56.50</b>
Wg+Fp+St (2)	<b>1.726</b>	<b>4.025</b>	<b>11.99</b>	<b>15.09</b>	<b>20.84</b>	<b>23.30</b>	<b>30.02</b>	<b>34.61</b>	<b>38.18</b>	<b>40.94</b>
Wg+Fp+Eg (4)	<b>2.413</b>	<b>4.750</b>	<b>9.615</b>	<b>13.00</b>	<b>19.39</b>	<b>23.43</b>	<b>25.18</b>	<b>25.97</b>	<b>30.75</b>	<b>31.87</b>
Wg+Eg+St+Ms (3)	<b>1.713</b>	<b>4.528</b>	<b>11.39</b>	<b>15.94</b>	<b>26.86</b>	<b>33.55</b>	<b>33.88</b>	<b>42.02</b>	<b>49.19</b>	<b>56.04</b>
Wg+Fp+Eg+St (4)	<b>1.707</b>	<b>3.914</b>	<b>8.412</b>	<b>11.49</b>	<b>18.88</b>	<b>20.49</b>	<b>21.83</b>	<b>24.16</b>	<b>29.03</b>	<b>31.35</b>
Wg+Fp+Eg+St+Ms (6)	<b>1.668</b>	<b>3.844</b>	<b>8.354</b>	<b>11.39</b>	<b>18.82</b>	<b>20.21</b>	<b>21.27</b>	<b>23.95</b>	<b>28.78</b>	<b>31.16</b>

mass and therefore, the presence of the engine will play a more significant role to higher modes whose deformation near the wing root become more and more important in higher natural modes.

- (iii) The same mass attached to the wing tip (store) exerts more significant effects on the natural frequencies than that attached closer to the wing root (missile), both for lower and higher modes, which is expected.

It is well-known that the fundamental natural modes play a vital role for the structural vibration such as in aeroelastic analysis whereas the higher natural modes are very important in other applications, e.g., acoustic transmission and noise control. The current method proposes an efficient and accurate tool to design and optimise an aircraft wing in the conceptual design phase. The superiority of the SDSM over other method like the FEM is clearly evident. Essential benefits are clearly low computational cost and high accuracy of results. The analytical essence of the methodology facilitates parametric and optimisation studies by varying significant structural parameters.

#### 4. Conclusions

An exact spectral dynamic stiffness (SDS) theory has been developed for free vibration analysis of composite plate-like structures with arbitrary non-uniform elastic supports, mass attachments as well as elastic coupling constraints. The principal conclusions are:

- (i) By using the modified Fourier series, the spectral dynamic stiffness (SDS) matrices for any arbitrarily distributed elastic supports, mass attachments

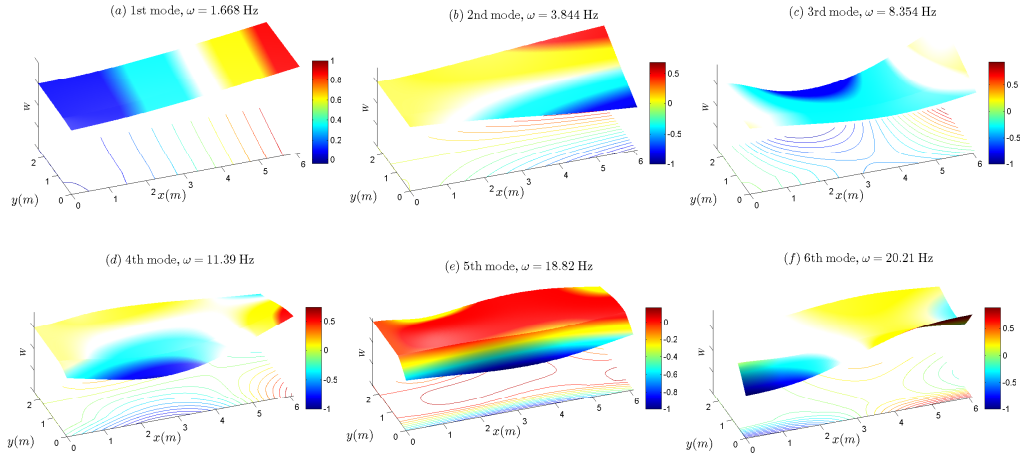


Figure 7: The first six natural modes of a laminated Goland wing made of Carbon fibre/epoxy and with store, missile, engine amounted as well as an elastically coupled flap (corresponding to the last case Wg+Fp+Eg+St+Ms in Table 10, only the wing and the flap are plotted out).

and elastic coupling constraints are formulated analytically in an exact sense in exact conformity with the SDSM for composite plate assemblies. The method has an exceedingly fast convergence rate and it gives exact solutions with high computational efficiency. The strong orthogonality of the adopted modified Fourier series and the elegant formulation procedure of SDS matrices ensures that there is no numerical instability problem in the computation. Therefore, any higher order Fourier series solution can be adopted during the computation to compute results to any desired accuracy.

- (ii) The method has no limitation when considering any combinations of translational and rotational elastic supports, mass attachments with/without rotatory inertia and elastic coupling constraints. This research fills a gap in literature to deal with non-uniformly distributed elastic supports and/or mass attachments and/or elastic coupling constraints for plate-like structures which have without doubt a wide range of applications in engineering.
- (iii) The analytical expressions for the dimensionless SDS matrices  $\mathbf{G}^a$  for any given dimensionless distribution functions  $G^a(\xi)$ ,  $\xi \in [-L, L]$  are formulated using a unified approach and the formulation needs to be performed only once for all. Consequently, the SDS formulation for any combination of the previous given  $G^a(\xi)$  can be directly obtained just by superposing the related  $\mathbf{G}^a$  which have already been formulated. Moreover, the same formulation  $\mathbf{G}^a$  can be applied to either translational or rotational deformations, for any combination of non-uniform elastic supports, elastic coupling constraints and mass attachments with/without the inclusion of rotatory inertia.
- (iv) The SDS matrices developed for non-uniform elastic supports and/or mass

1  
2  
3  
4  
5 attachments and/or elastic coupling constraints are superposed directly onto  
6 the unmodified SDS matrix of a plate assembly. The procedure is in a strong  
7 form and no extra DOF is introduced in the final SDS matrices and therefore,  
8 no extra computational effort is required. Additionally, in this procedure, no  
9 penalty parameter is used and the shortcomings of the penalty method are  
10 completely avoided.

- 11  
12  
13 (v) The development retains all significant advantages of the SDSM [27–29],  
14 including the unprecedented efficiency, accuracy and robustness. More im-  
15 portantly, the research has extended the SDSM theory to deal with much  
16 more general composite plate-like structures with arbitrarily distributed elas-  
17 tic supports, elastic coupling constraints as well as arbitrary non-uniform  
18 mass attachments along any of the line nodes. Novel possibilities of exact  
19 modal analysis for practical composite plate-like structures in a more general  
20 manner have opened up as a results of this research.  
21  
22  
23 (vi) The theory presented in this paper is completely general which can be ap-  
24 plied to both SDSM and DSM formulations based on different governing  
25 differential equations. Furthermore, it can be applied to modal as well as  
26 dynamic response analyses.  
27  
28  
29

### 30 **Appendix A. The analytical expressions of $G^a$ matrices for some typical func-** 31 **tions**

32  
33 The analytical expressions of dimensionless SDS matrices  $G^a$  for any given  
34 distribution function  $G^a(\xi)$  can be easily derived based on Eq. (15) by symbolic  
35 calculation. However, this appendix includes the analytical expressions of the  
36  $G^a$  matrices only for some typical distribution functions  $G^a(\xi)$ . For the sake of  
37 notational convenience, some notations are introduced. If  $S$  terms are adopted in  
38 the series solution ( $s \in [0, S - 1]$ ), then  $\text{diag}(\cdot)_{S^0}$  is used to denote a diagonal  
39 matrix with the ‘s’ in expression ‘.’ taking  $s \in [0, S - 1]$ , also  $\text{diag}(\cdot)_{S^1}$  with ‘.’  
40 taking  $s \in [1, S - 1]$ . Similarly,  $[\cdot]_{0,S^1}$  stands for a row vector with ‘.’ taking  $r = 0$   
41 and  $s \in [1, S - 1]$ ;  $[\cdot]_{S^1,0}$  represents a column vector with ‘.’ taking  $r \in [1, S -$   
42  $1]$ ,  $s = 0$ ;  $[\cdot]_{S^1,S^1}$  denotes a matrix with ‘.’ taking  $r \in [1, S - 1]$ ,  $s \in [1, S - 1]$  and  
43 so on.  
44  
45  
46

47 As mentioned earlier, for symmetric distribution functions  $G^a(\xi)$ ,  $\mathbf{G}_{01}^a = \mathbf{G}_{10}^a =$   
48  $\mathbf{O}$  whereas  $\mathbf{G}_{00}^a$  and  $\mathbf{G}_{11}^a$  are derived from Eq. (15), whose analytical expressions  
49 are given below for some typical symmetric (even) functions  $G^a(\xi)$ .  
50

- 51 (1) For constant function  $G^a(\xi) = 1$ ,  $\mathbf{G}_{00}^a = \mathbf{G}_{11}^a = \text{diag}(1)_{S^0}$ .  
52  
53  
54  
55  
56  
57  
58  
59  
60  
61  
62  
63  
64  
65

(2) For parabolic function  $G^a(\xi) = (\xi/L)^2$ ,

$$\mathbf{G}_{00}^a = \begin{bmatrix} \frac{1}{3} & \left[ \frac{2\sqrt{2}(-1)^s}{(\pi s)^2} \right]_{0, S^1} \\ \left[ \frac{2\sqrt{2}(-1)^r}{(\pi r)^2} \right]_{S^1, 0} & \left[ \frac{4(-1)^{r+s}(r^2+s^2)}{(\pi(r^2-s^2))^2} \right]_{S^1, S^1} \end{bmatrix}$$

except for the diagonal terms  $\mathbf{G}_{00}^a(r+1, s+1) = [1/3 + 1/(2\pi^2 s^2)]$  for  $r = s \in [1, S-1]$ ; and  $\mathbf{G}_{11}^a = \left[ \frac{2(-1)^{r+s}(1+2r(1+r)+2s(1+s))}{(\pi(r-s)(1+r+s))^2} \right]_{S^0, S^0}$  except for the diagonal terms  $\mathbf{G}_{11}^a(r+1, s+1) = [1/3 + 2/(\pi s_2)^2]$  for  $r = s \in [0, S-1]$  and where  $s_2 = 1 + 2s$ .

(3) For cosine function  $G^a(\xi) = \cos(\pi\xi/(2L))$ ,

$$\mathbf{G}_{00}^a = \begin{bmatrix} \frac{2}{\pi} & \left[ \frac{2\sqrt{2}(-1)^s}{\pi(1-4s^2)} \right]_{0, S^1} \\ \left[ \frac{2\sqrt{2}(-1)^r}{\pi(1-4r^2)} \right]_{S^1, 0} & \left[ \frac{4(-1)^{r+s}(1-4r^2-4s^2)}{\pi(16r^4+(1-4s^2)^2-8r^2(1+4s^2))} \right]_{S^1, S^1} \end{bmatrix}$$

except for the diagonal terms  $\mathbf{G}_{00}^a(r+1, s+1) = (4 - 32s^2)/[\pi(1 - 16s^2)]$  for  $r = s \in [1, S-1]$ ; and

$$\mathbf{G}_{11}^a = \left[ \frac{4(-1)^{r+s}(4r(1+r) + (1+2s)^2)}{\pi(4(r-s)^2 - 1)(1+2r+2s)(3+2r+2s)} \right]_{S^0, S^0}$$

except for the diagonal terms  $\mathbf{G}_{11}^a(r+1, s+1) = 4(1+8s(1+s))/[\pi(1+4s)(3+4s)]$  for  $r = s \in [0, S-1]$ .

For antisymmetric distribution functions  $G^a(\xi)$ ,  $\mathbf{G}_{00}^a = \mathbf{G}_{11}^a = \mathbf{O}$  whereas  $\mathbf{G}_{01}^a$  and  $\mathbf{G}_{10}^a$  are derived from Eq. (15), whose analytical expressions are given below for some typical antisymmetric (odd) functions  $G^a(\xi)$ .

(1) For linear function  $G^a(\xi) = \xi/L$ ,  $\mathbf{G}_{00}^a = \mathbf{G}_{11}^a = \mathbf{O}$  and

$$\mathbf{G}_{10}^{aT} = \mathbf{G}_{01}^a = \begin{bmatrix} [4\sqrt{2}(-1)^s/(\pi s_2)^2]_{0, S^0} \\ \left[ 8(-1)^{r+s}(4r^2 + s_2^2)/(\pi(-4r^2 + s_2^2))^2 \right]_{S^1, S^0} \end{bmatrix}$$

(2) For sine function  $G^a(\xi) = \sin(\pi\xi/(2L))$ ,  $\mathbf{G}_{01}^a = \mathbf{G}_{10}^a = \text{diag}(1/2)_{S^0}$ .

## Acknowledgements

The authors appreciate the support given by EPSRC, UK through a Grant EP/J007706/1 which made this work possible.

## References

- [1] H. G. D. Goyder, R. G. White, Vibrational power flow from machines into built-up structures, Part I: Introduction and approximate analyses of beam and plate-like foundations, *Journal of Sound and Vibration* 68 (1) (1980) 59–75. doi:10.1016/0022-460X(80)90452-6.
- [2] N. Levy, J. R. Rice, The part-through surface crack in an elastic plate, *Journal of Applied Mechanics* 39 (1) (1972) 185–194. doi:10.1115/1.3422609.
- [3] M. Sari, M. Nazari, E. A. Butcher, Effects of Damaged Boundaries on the Free Vibration of Kirchhoff Plates: Comparison of Perturbation and Spectral Collocation Solutions, *Journal of Computational and Nonlinear Dynamics* 7 (1) (2012) 011011. doi:10.1115/1.4004808.
- [4] D. Zhou, Natural frequencies of elastically restrained rectangular plates using a set of static beam functions in the Rayleigh-Ritz method, *Computers & Structures* 57 (4) (1995) 731–735. doi:10.1016/0045-7949(95)00066-P.
- [5] R. O. Grossi, R. B. Bhat, Natural frequencies of edge restrained tapered rectangular plates, *Journal of Sound and Vibration* 185 (2) (1995) 335–343. doi:10.1006/jsvi.1995.0382.
- [6] Y. K. Cheung, D. Zhou, Vibrations of rectangular plates with elastic intermediate line-supports and edge constraints, *Thin-Walled Structures* 37 (2000) 305–331. doi:10.1016/S0263-8231(00)00015-X.
- [7] L. Dozio, On the use of the Trigonometric Ritz method for general vibration analysis of rectangular Kirchhoff plates, *Thin-Walled Structures* 49 (1) (2011) 129–144. doi:10.1016/j.tws.2010.08.014.
- [8] S. A. Eftekhari, A. A. Jafari, Accurate variational approach for free vibration of variable thickness thin and thick plates with edges elastically restrained against translation and rotation, *International Journal of Mechanical Sciences* 68 (2013) 35–46. doi:10.1016/j.ijmecsci.2012.12.012.
- [9] W. L. Li, Vibration analysis of rectangular plates with general elastic boundary supports, *Journal of Sound and Vibration* 273 (3) (2004) 619–635. doi:10.1016/S0022-460X(03)00562-5.

- 1  
2  
3  
4  
5 [10] H. Khov, W. L. Li, R. F. Gibson, An accurate solution method for the static  
6 and dynamic deflections of orthotropic plates with general boundary condi-  
7 tions, *Composite Structures* 90 (4) (2009) 474–481. doi:10.1016/j.  
8 compstruct.2009.04.020.  
9  
10 [11] I. E. Harik, X. Liu, N. Balakrishnan, Analytic solution to free vibration of  
11 rectangular plates, *Journal of sound and vibration* 153 (1) (1992) 51–62.  
12 doi:10.1016/0022-460X(92)90626-9.  
13  
14 [12] A. S. Ashour, Vibration of angle-ply symmetric laminated composite plates  
15 with edges elastically restrained, *Composite Structures* 74 (2006) 294–302.  
16 doi:10.1016/j.compstruct.2006.07.012.  
17  
18 [13] A. W. Leissa, P. A. A. Laura, R. H. Gutierrez, Vibrations of Rectangular  
19 Plates With Nonuniform Elastic Edge supports, *Journal of Applied Mechanics*  
20 47 (1980) 891–895. doi:10.1115/1.3153809.  
21  
22 [14] P. A. A. Laura, R. H. Gutierrez, Analysis of Vibrating Rectangular Plates  
23 With Non-Uniform Boundary Conditions By Using the Differential Quadra-  
24 ture Method, *Journal of Sound and Vibration* 173 (5) (1994) 702–706.  
25 doi:10.1006/jsvi.1994.1255.  
26  
27 [15] D. J. Gorman, A general solution for the free vibration of rectangular plates  
28 with arbitrarily distributed lateral and rotational elastic edge support, *Journal*  
29 *of Sound and Vibration* 174 (4) (1994) 451–459. doi:10.1006/jsvi.  
30 1994.1287.  
31  
32 [16] C. Shu, C. M. Wang, Treatment of mixed and nonuniform boundary condi-  
33 tions in GDQ vibration analysis of rectangular plates, *Engineering Structures*  
34 21 (1999) 125–134. doi:10.1016/S0141-0296(97)00155-7.  
35  
36 [17] Y. B. Zhao, G. W. Wei, DSC Analysis of Rectangular Plates With Non-  
37 Uniform Boundary Conditions, *Journal of Sound and Vibration* 255 (2)  
38 (2002) 203–228. doi:10.1006/jsvi.2001.4150.  
39  
40 [18] X. Zhang, W. L. Li, Vibrations of rectangular plates with arbitrary non-  
41 uniform elastic edge restraints, *Journal of Sound and Vibration* 326 (2009)  
42 221–234. doi:10.1016/j.jsv.2009.04.021.  
43  
44 [19] D. J. Gorman, A general solution for the free vibration of rectangular plates  
45 resting on uniform elastic edge supports, *Journal of Sound and Vibration*  
46 139 (2) (1990) 325–335. doi:10.1016/0022-460X(90)90893-5.  
47  
48  
49  
50  
51  
52  
53  
54  
55  
56  
57  
58  
59  
60  
61  
62  
63  
64  
65

- 1  
2  
3  
4  
5 [20] Y. C. Das, D. R. Navaratna, Vibrations of a rectangular plate with con-  
6 centrated mass, spring, and dashpot, *Journal of Applied Mechanics* 30 (1)  
7 (1963) 31–36. doi:10.1016/0016-0032(56)90017-5.  
8  
9  
10 [21] M. Chiba, T. Sugimoto, Vibration characteristics of a cantilever plate with  
11 attached spring-mass system, *Journal of Sound and Vibration* 260 (2) (2003)  
12 237–263. doi:10.1016/S0022-460X(02)00921-5.  
13  
14 [22] S. D. Yu, Free and forced flexural vibration analysis of cantilever plates with  
15 attached point mass, *Journal of Sound and Vibration* 321 (1-2) (2009) 270–  
16 285. doi:10.1016/j.jsv.2008.09.042.  
17  
18 [23] R. J. Watkins, S. Santillan, J. Radice, O. Barton, Vibration response of an  
19 elastically point-supported plate with attached masses, *Thin-Walled Struc-*  
20 *tures* 48 (7) (2010) 519–527. doi:10.1016/j.tws.2010.02.005.  
21  
22 [24] Q. S. Li, Vibratory characteristics of multistep nonuniform orthotropic shear  
23 plates with line spring supports and line masses, *The Journal of the Acous-*  
24 *tical Society of America* 110 (3) (2001) 1360–1370. doi:10.1121/1.  
25 1387995.  
26  
27 [25] Q. S. Li, An exact approach for free vibration analysis of rectangular plates  
28 with line-concentrated mass and elastic line-support, *International Jour-*  
29 *nal of Mechanical Sciences* 45 (4) (2003) 669–685. doi:10.1016/  
30 S0020-7403(03)00110-3.  
31  
32 [26] J. Du, W. L. Li, Z. Liu, T. Yang, G. Jin, Free vibration of two elastically  
33 coupled rectangular plates with uniform elastic boundary restraints, *Journal*  
34 *of Sound and Vibration* 330 (4) (2011) 788–804. doi:10.1016/j.jsv.  
35 2010.08.044.  
36  
37 [27] X. Liu, J. R. Banerjee, Free vibration analysis for plates with arbi-  
38 trary boundary conditions using a novel spectral-dynamic stiffness method,  
39 *Computers & Structures* 164 (2016) 108–126. doi:10.1016/j.  
40 compstruc.2015.11.005.  
41  
42 [28] X. Liu, J. R. Banerjee, An exact spectral-dynamic stiffness method for free  
43 flexural vibration analysis of orthotropic composite plate assemblies - Part I:  
44 Theory, *Composite Structures* 132 (2015) 1274–1287. doi:10.1016/j.  
45 compstruct.2015.07.020.  
46  
47 [29] X. Liu, J. R. Banerjee, An exact spectral-dynamic stiffness method for free  
48 flexural vibration analysis of orthotropic composite plate assemblies - Part  
49  
50  
51  
52  
53  
54  
55  
56  
57  
58  
59  
60  
61  
62  
63  
64  
65

- 1  
2  
3  
4  
5 II: Applications, Composite Structures (132) (2015) 1288–1302. doi:10.  
6 1016/j.compstruct.2015.07.022.  
7  
8 [30] A. Iserles, S. P. Nørsett, From high oscillation to rapid approximation I:  
9 Modified Fourier expansions, IMA Journal of Applied Mathematics 28 (4)  
10 (2006) 862–887. doi:10.1093/imanum/drn006.  
11  
12 [31] X. Liu, J. Banerjee, Spectral dynamic stiffness formulation for free vibration  
13 analysis of plane elasticity problems (in preparation) (2016).  
14  
15 [32] M. Boscolo, J. R. Banerjee, Dynamic stiffness elements and their applica-  
16 tions for plates using first order shear deformation theory, Computers &  
17 Structures 89 (3-4) (2011) 395–410. doi:10.1016/j.compstruc.  
18 2010.11.005.  
19  
20 [33] M. Boscolo, J. R. Banerjee, Dynamic stiffness formulation for compos-  
21 ite Mindlin plates for exact modal analysis of structures. Part I: The-  
22 ory, Computers & Structures 96-97 (2012) 61–73. doi:10.1016/j.  
23 compstruc.2012.01.002.  
24  
25 [34] F. A. Fazzolari, M. Boscolo, J. R. Banerjee, An exact dynamic stiffness ele-  
26 ment using a higher order shear deformation theory for free vibration analy-  
27 sis of composite plate assemblies, Composite Structures 96 (2013) 262–278.  
28 doi:10.1016/j.compstruct.2012.08.033.  
29  
30 [35] M. Boscolo, J. R. Banerjee, Layer-wise dynamic stiffness solution for free  
31 vibration analysis of laminated composite plates, Journal of Sound and Vi-  
32 bration 333 (1) (2014) 200–227. doi:10.1016/j.jsv.2013.08.  
33 031.  
34  
35 [36] A. Pagani, E. Carrera, J. R. Banerjee, P. H. Cabral, G. Caprio, A. Prado, Free  
36 vibration analysis of composite plates by higher-order 1D dynamic stiff-  
37 ness elements and experiments, Composite Structures 118 (2014) 654–663.  
38 doi:10.1016/j.compstruct.2014.08.020.  
39  
40 [37] W. X. Zhong, Duality System in Applied Mechanics and Optimal Control,  
41 Kluwer Academic Publishers, London, 2004.  
42  
43 [38] J. N. Reddy, Mechanics of laminated composite plates and shells Theory and  
44 analysis, 2nd Edition, CRC Press, 2003.  
45  
46 [39] P. S. Beran, T. W. Strganac, K. Kim, C. Nichkawde, Studies of store-  
47 induced limit-cycle oscillations using a model with full system nonlinear-  
48 ities, Nonlinear Dynamics 37 (4) (2004) 323–339. doi:10.1023/B:  
49 NODY.0000045544.96418.bf.  
50  
51  
52  
53  
54  
55  
56  
57  
58  
59  
60  
61  
62  
63  
64  
65

1  
2  
3  
4  
5  
6  
7  
8  
9  
10  
11  
12  
13  
14  
15  
16  
17  
18  
19  
20  
21  
22  
23  
24  
25  
26  
27  
28  
29  
30  
31  
32  
33  
34  
35  
36  
37  
38  
39  
40  
41  
42  
43  
44  
45  
46  
47  
48  
49  
50  
51  
52  
53  
54  
55  
56  
57  
58  
59  
60  
61  
62  
63  
64  
65

[40] C. Chung, S. Shin, Worst Case Flutter Analysis of a Stored Wing with Structural and Aerodynamic Variation, in: 51st AIAA/ASME/ASCE/AHS/ASC Structures, Structural Dynamics, and Materials Conference, Orlando, Florida, 2010, pp. 2010–2803.

[41] J. R. Banerjee, X. Liu, H. I. Kassem, Aeroelastic stability analysis of high aspect ratio aircraft wings, *Journal of Applied Nonlinear Dynamics* 3 (4) (2014) 413–422. doi:10.5890/JAND.2014.12.012.

[42] H. I. Kassem, X. Liu, J. R. Banerjee, Transonic flutter analysis using a fully coupled density based solver for inviscid flow (under review), *Advances in Engineering Software*.

[43] M. Goland, The flutter of a uniform cantilever wing, *Journal of Applied Mechanics* 12 (4) (1945) A197–A208.

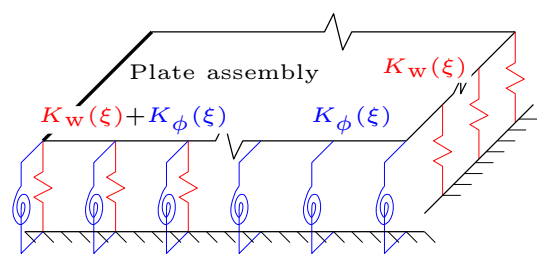
Latex source file

[Click here to download LaTeX Source Files: COST2015c.tex](#)

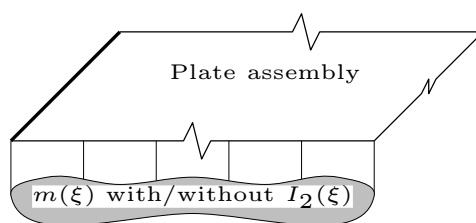
**bibtex file for Latex**

**[Click here to download LaTeX Source Files: SpringMassAttachments.bib](#)**

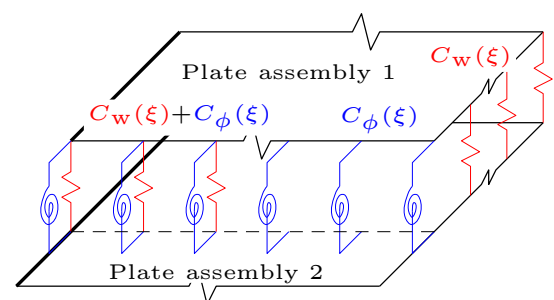
Figure 1



(a) Elastic supports



(b) Mass attachments



(c) Elastic coupling constraints

Figure 2

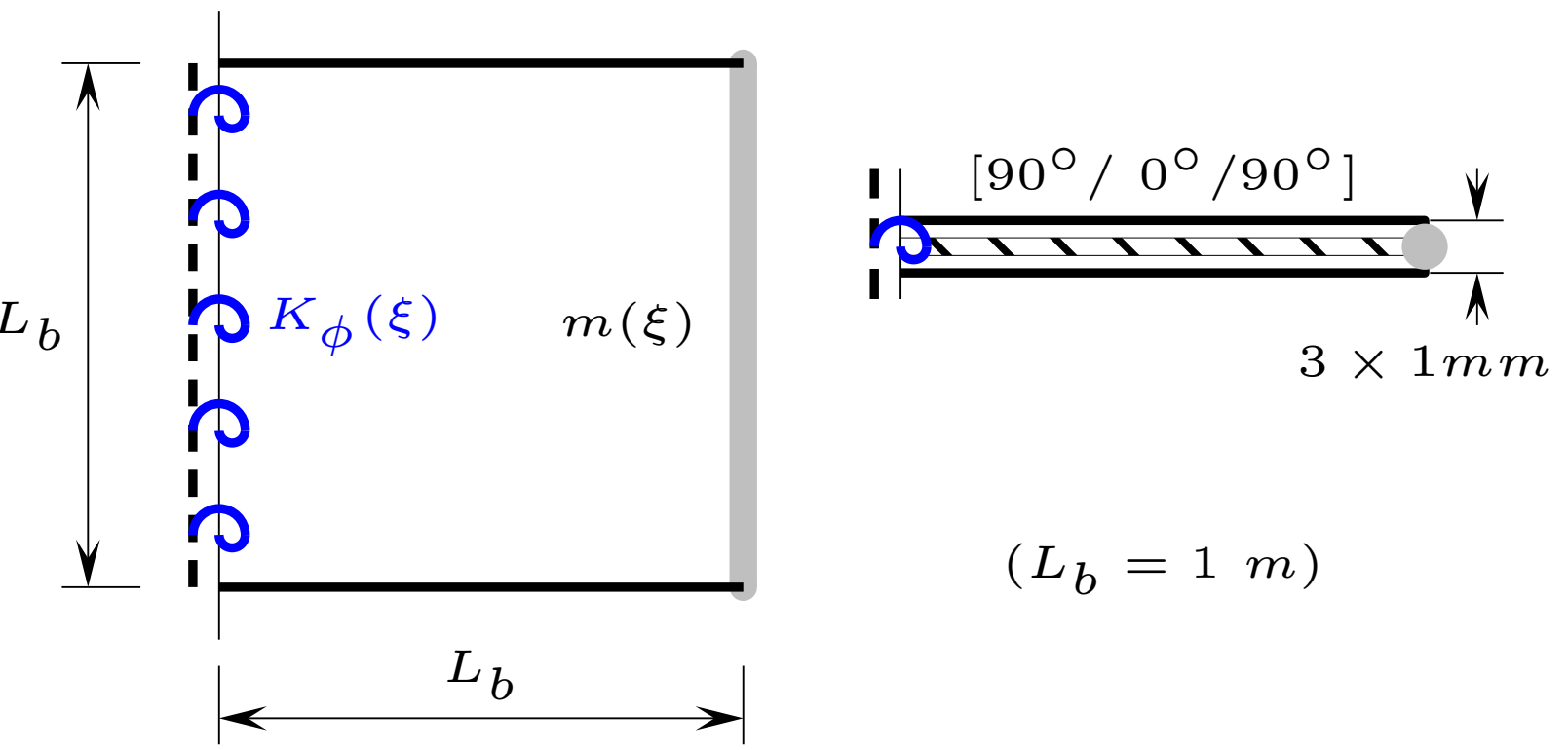


Figure 3a

(a) Case 2, 1st mode,  $\omega = 0.89976$  Hz

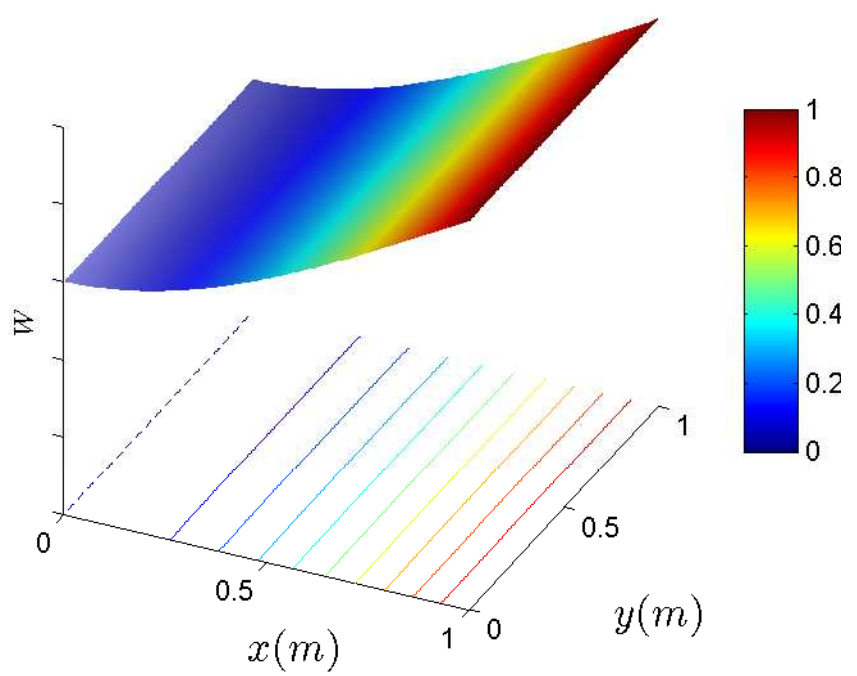


Figure 3b

(b) Case 2, 2nd mode,  $\omega = 2.5774$  Hz

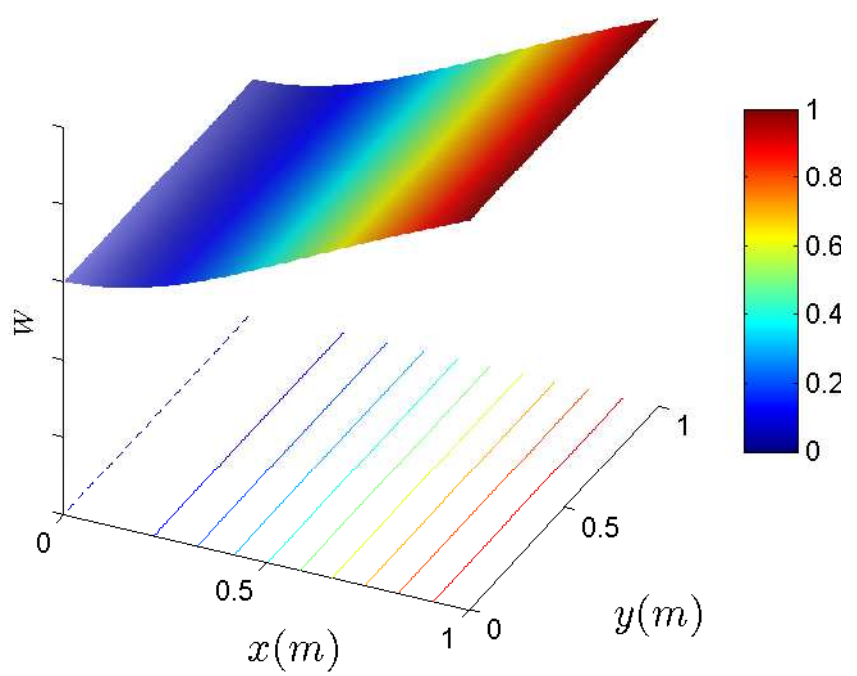


Figure 3c

(c) Case 2, 4th mode,  $\omega = 10.777$  Hz

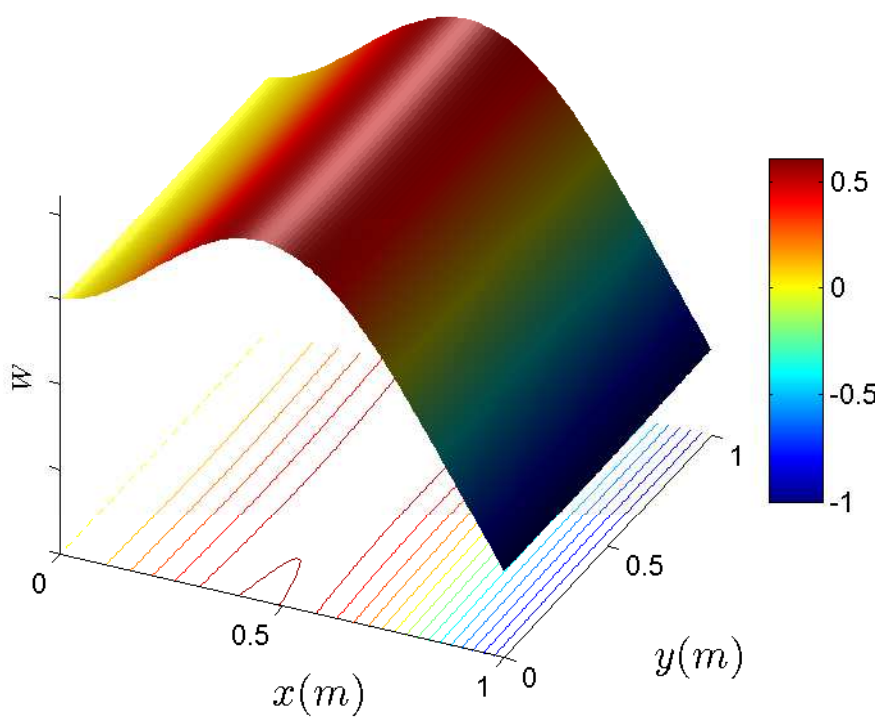


Figure 3d

(d) Case 4, 1st mode,  $\omega = 0.89115$  Hz

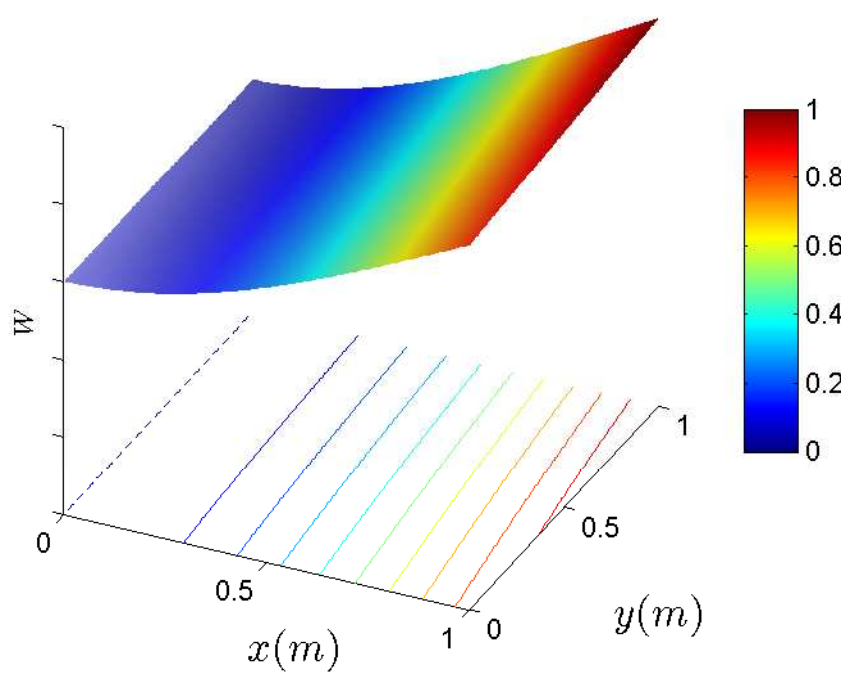
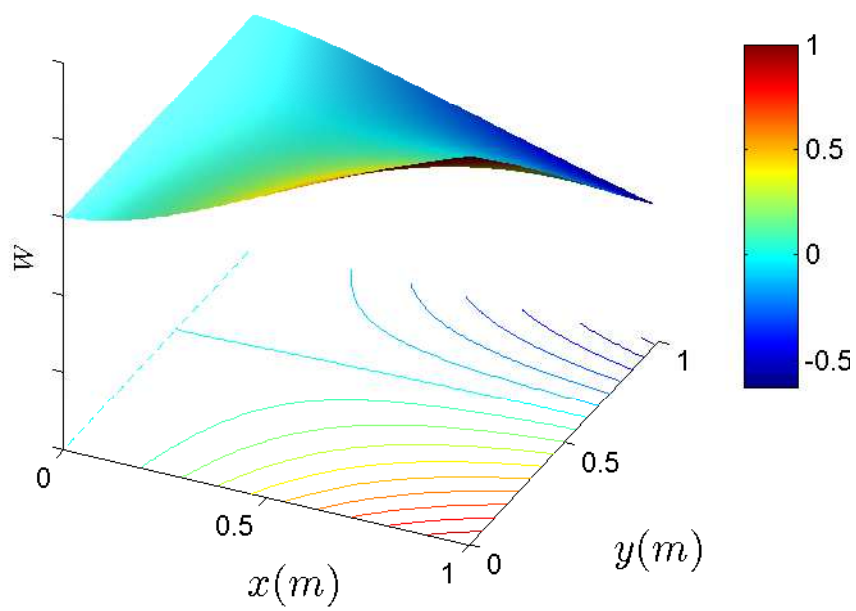


Figure 3e

(e) Case 4, 2nd mode,  $\omega = 2.7917$  Hz



(f) Case 4, 4th mode,  $\omega = 10.917$  Hz

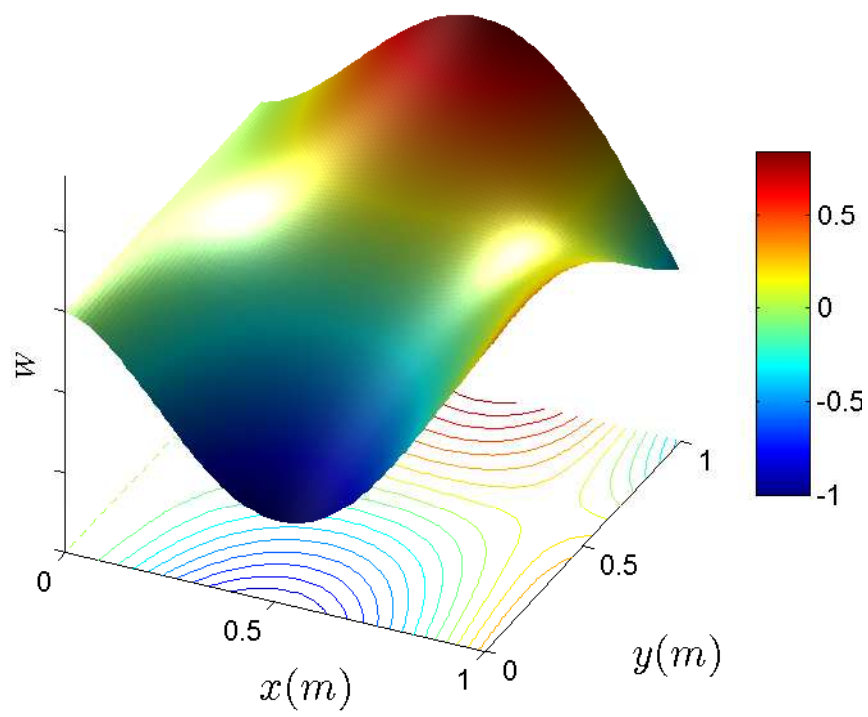


Figure 4

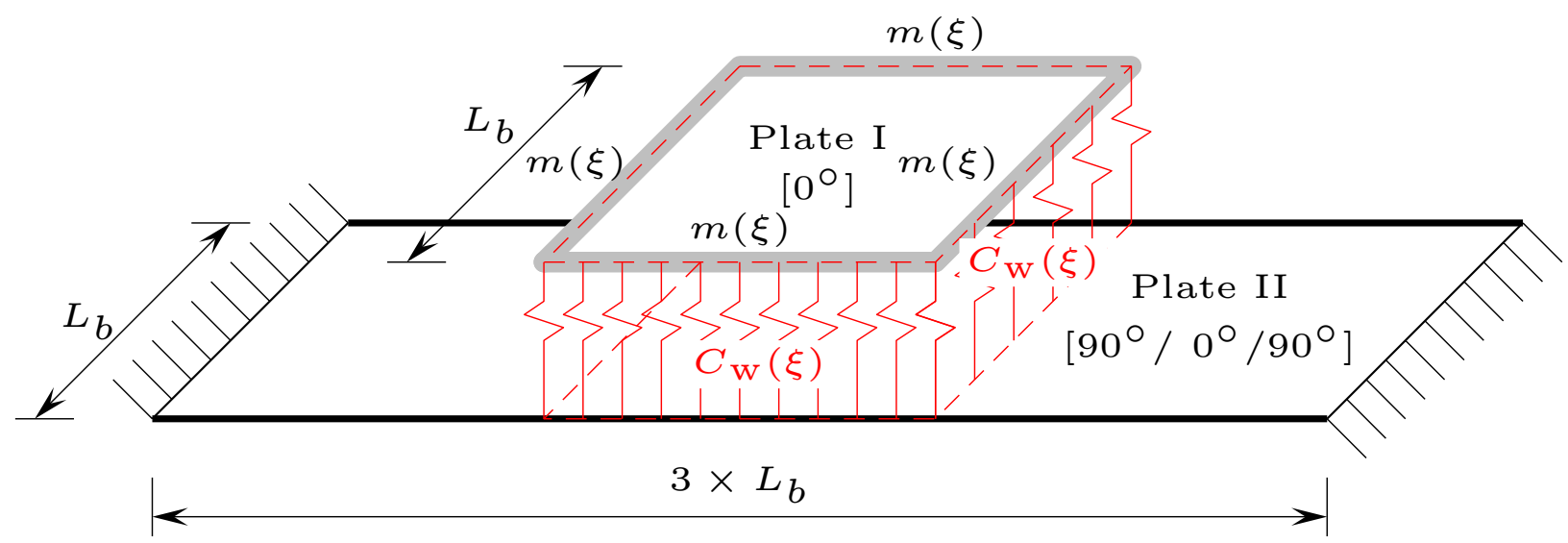


Figure 5a

2nd mode,  $\omega = 1.7889$  Hz

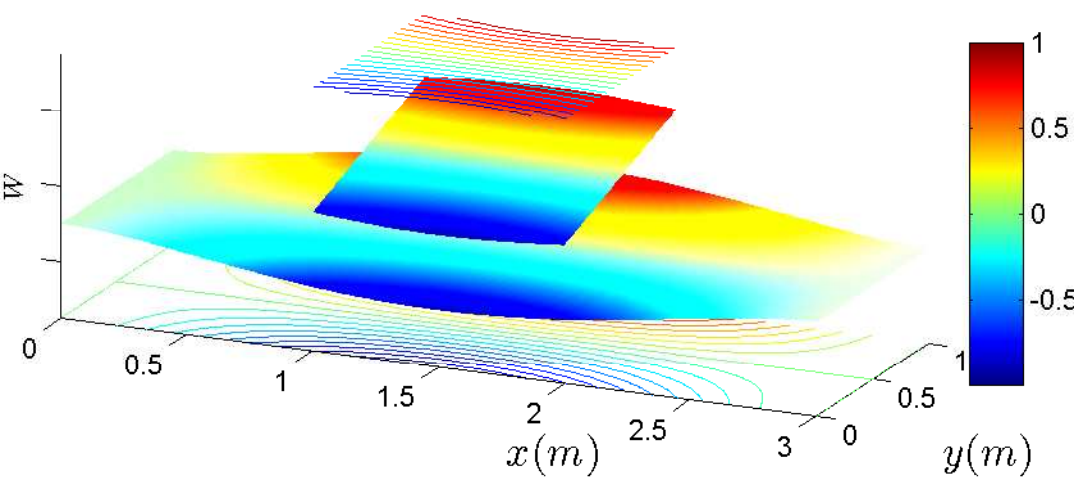


Figure 5b

3rd mode,  $\omega = 2.5854$  Hz

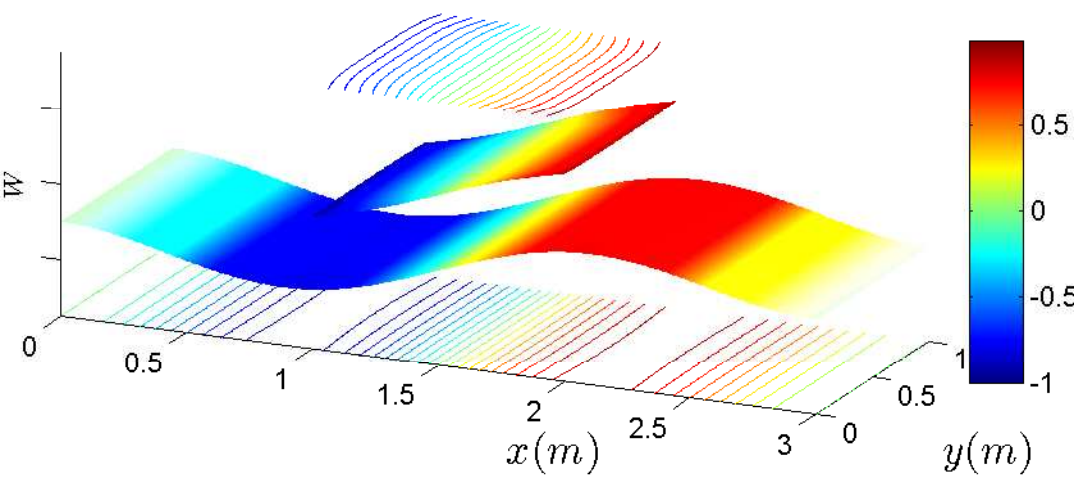


Figure 5c

5th mode,  $\omega = 5.3237$  Hz

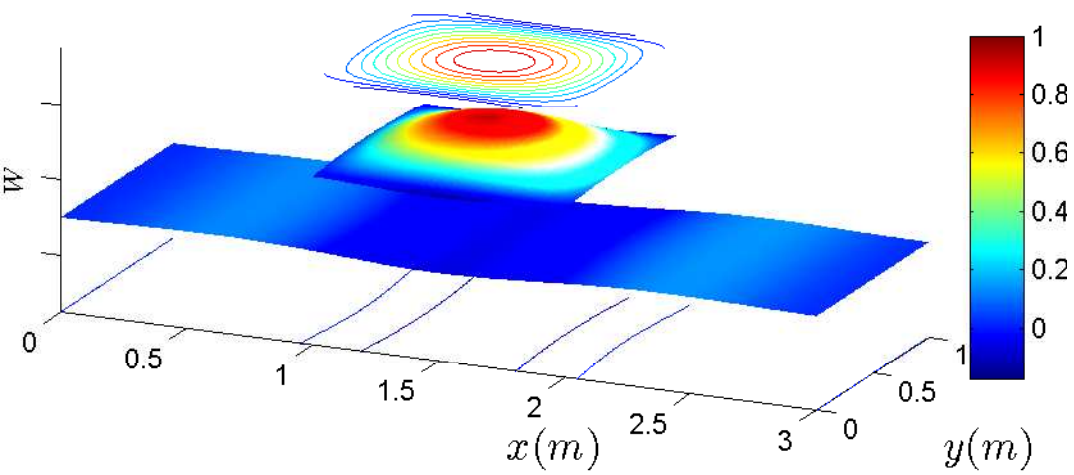


Figure 5d

20th mode,  $\omega = 16.485$  Hz

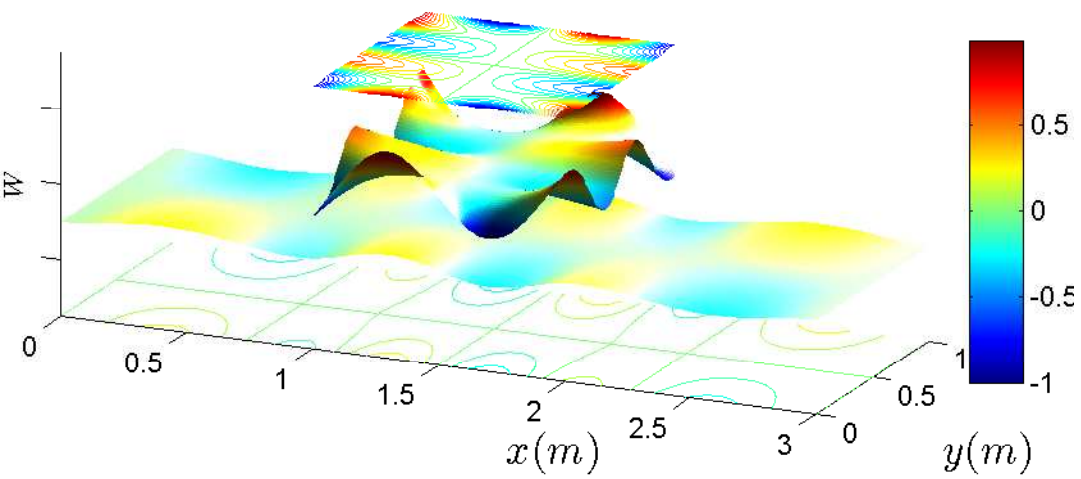


Figure 6

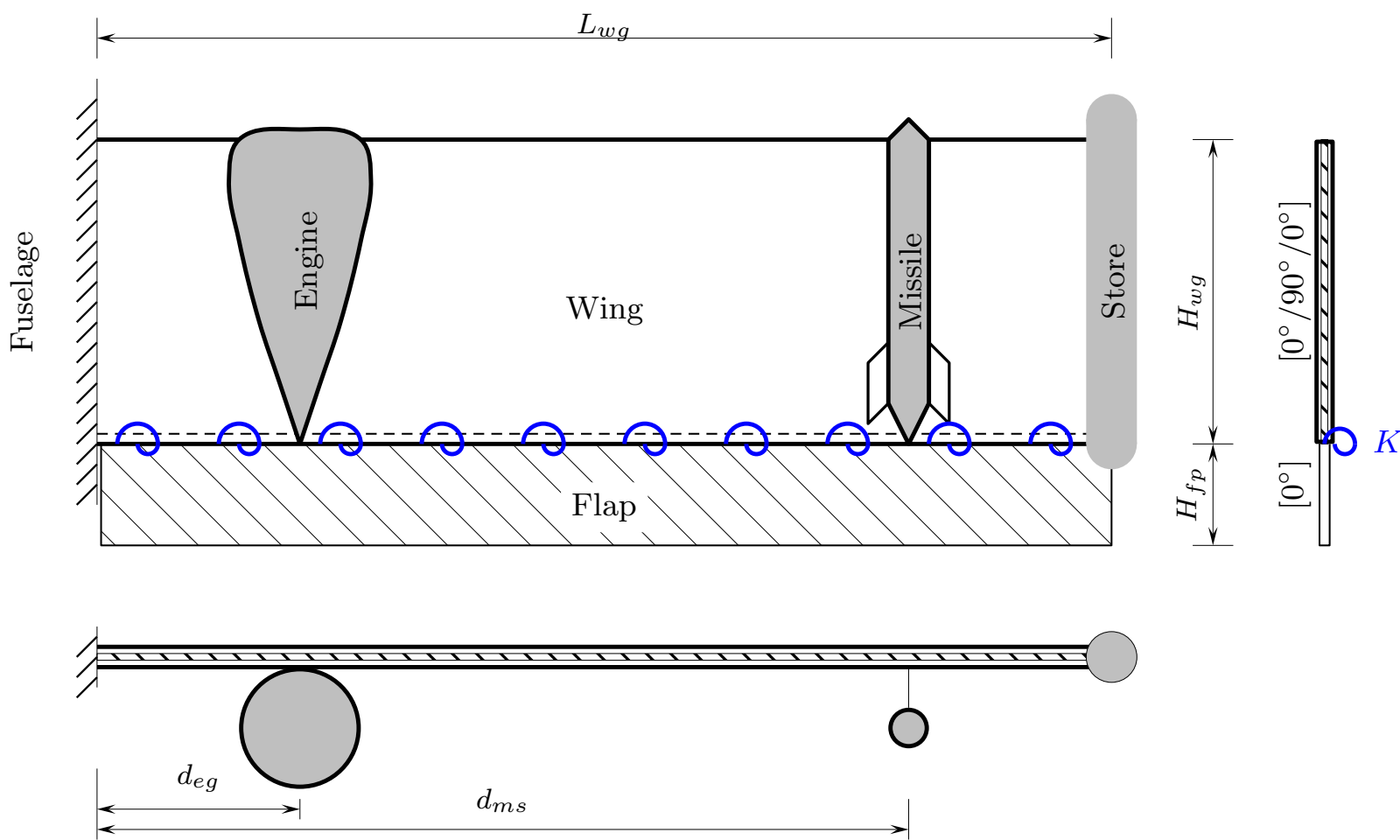


Figure 7a

(a) 1st mode,  $\omega = 1.668$  Hz

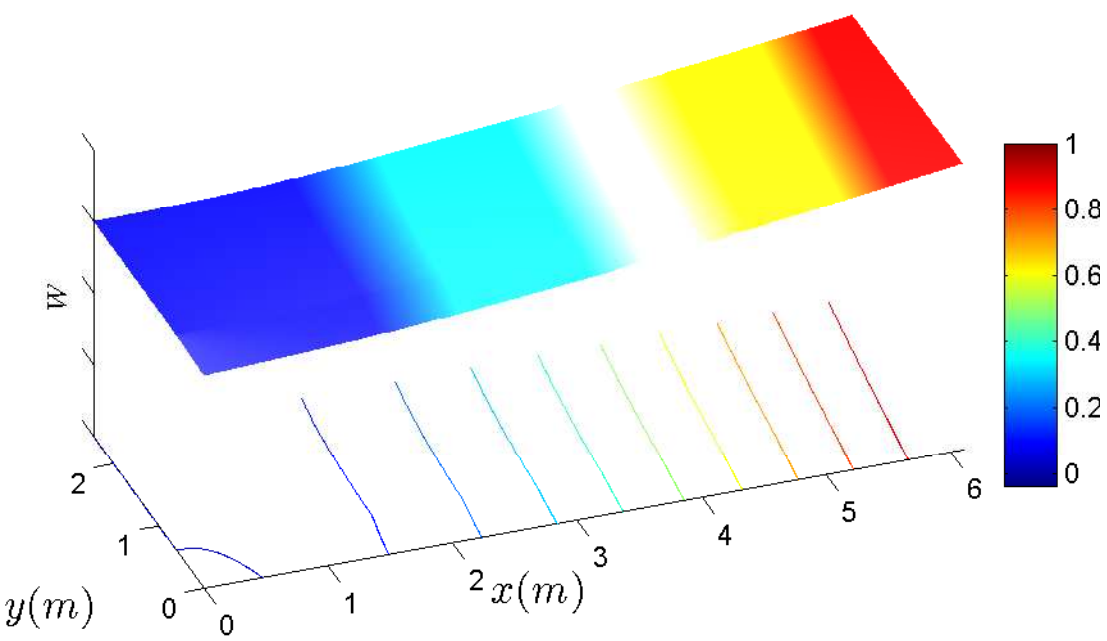


Figure 7b

(b) 2nd mode,  $\omega = 3.844$  Hz

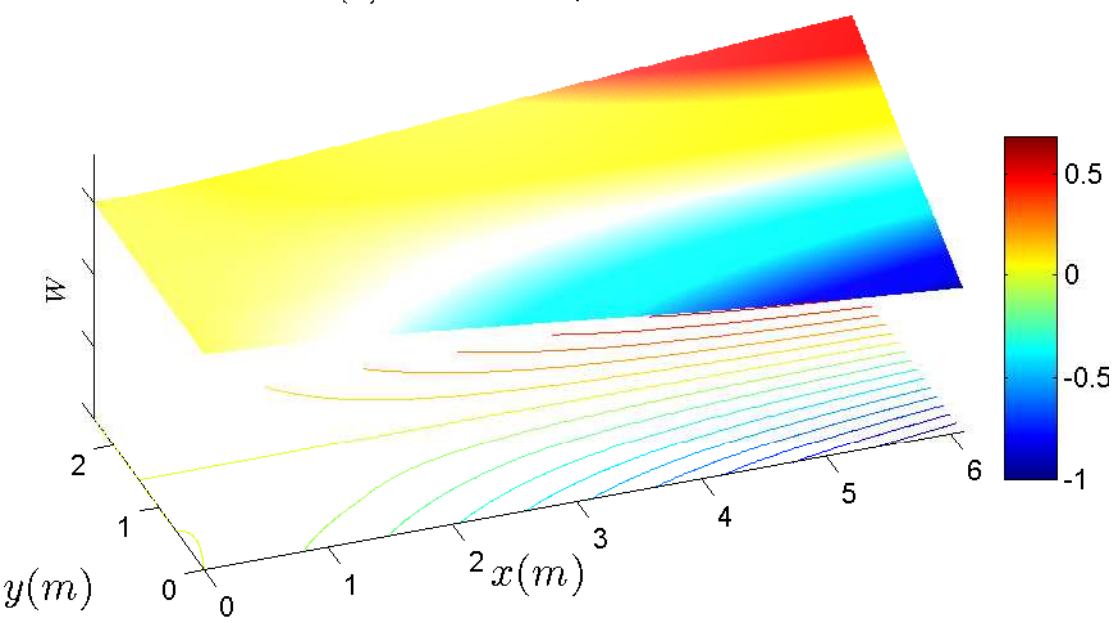


Figure 7c

(c) 3rd mode,  $\omega = 8.354$  Hz

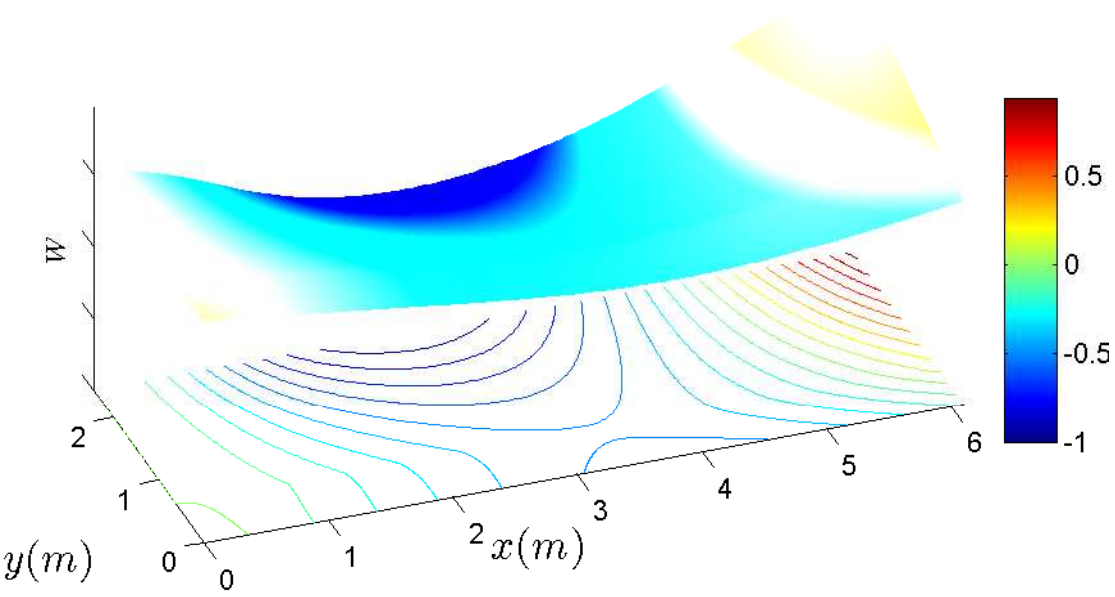


Figure 7d

(d) 4th mode,  $\omega = 11.39$  Hz

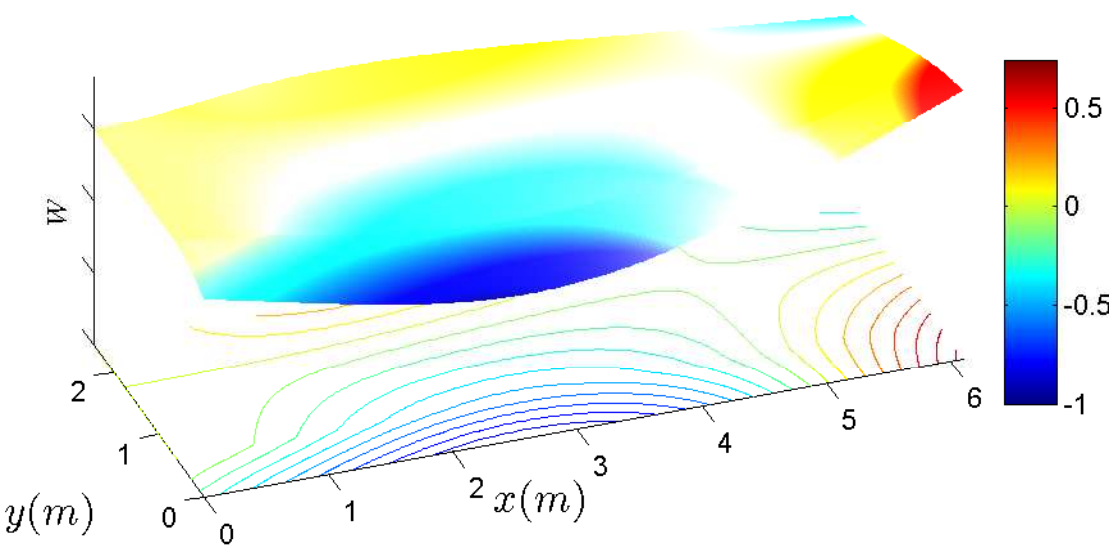


Figure 7e

(e) 5th mode,  $\omega = 18.82$  Hz

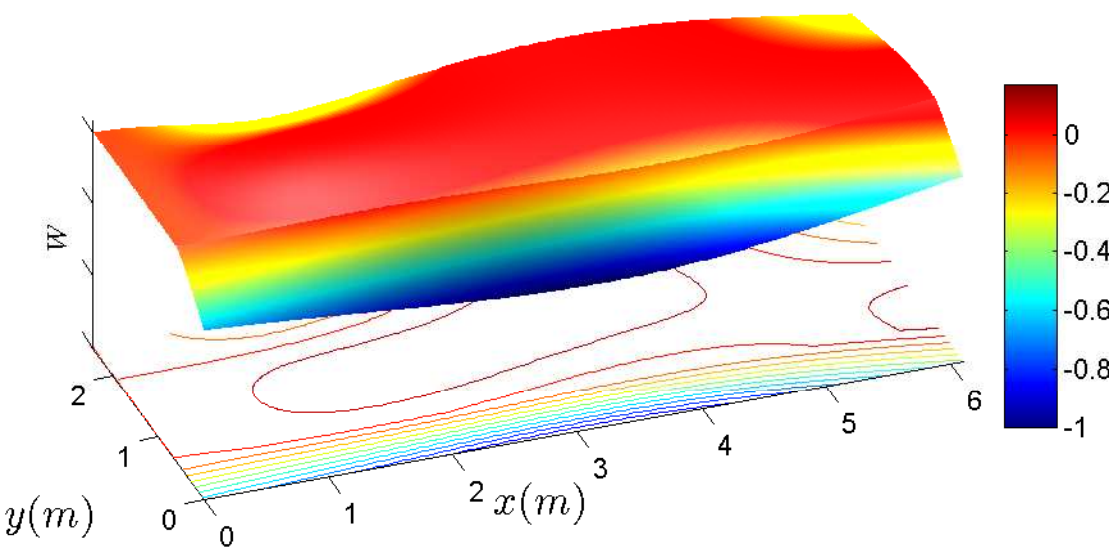


Figure 7f

(f) 6th mode,  $\omega = 20.21$  Hz

